

Stinging nettle (*Urtica dioica* L.) as reinforcement in short fibre-reinforced biobased composites for application in injection moulding – a possible use case for biomass from marginal land?

Jonas-Rumi Baumann[a], Lea Schönfeld[a], Carsten Lühr[b], Hans-Jörg Gusovius[b], Wajih Akleh[c], Jason Govilas[c], Vincent Placet[c], Michel Chalot[d, e] & Jörg Müssig[a, *]

[a] The Biological Materials Group, Dept. of Biomimetics, HSB - Hochschule Bremen - City University of Applied Sciences, Neustadtswall 30, Bremen 28199, Germany

[b] Leibniz Institute for Agricultural Engineering and Bioeconomy Potsdam-Bornim (ATB), Max-Eyth-Allee 100, 14469 Potsdam, Germany

[c] Université de Franche-Comté, CNRS, Institut FEMTO-ST, 25000, Besançon, France

[d] Université de Franche-Comté, CNRS, Chrono-Environnement, 25200 Montbéliard, France

[e] Université de Lorraine, Faculté des Sciences et Technologies, 54000, Nancy, France

Abstract

Stinging nettle (*Urtica dioica* L.) has been observed to grow spontaneously on metal-contaminated soils marginalised by heavy industrial use, thereby presenting an opportunity for the economic utilisation of such lands. This study explores the potential of nettle as a fibre crop by producing short-fibre reinforced polylactic acid (PLA) composites through compounding and injection moulding. Whole stem segments from three nettle clones (B13, L18, and Roville), along with separated fibre bundles from the L18 clone, were processed. The fibre bundles were separated using a roller breaker unit and a hammer mill. From separation with the hammer mill, not only cleaned fibre bundles but also the uncleaned fibre-shive mixture and the undersieve fraction were processed. The Young's modulus of all composites exceeded that of unreinforced PLA, with mean values ranging from 5.7 to 8.1 GPa. However, the tensile strength of most composites was lower than that of pure PLA, except for the two composites reinforced with cleaned fibre bundles. Of these two, the reinforcement with fibre bundles from separation with the hammer mill led to superior mechanical properties, with a higher Young's modulus (8.1 GPa) and tensile strength (61.8 MPa) compared to those separated using the breaking unit (7.2 GPa and 55.9 MPa). This enhancement is hypothesised to result from reduced fibre damage and lower fibre bundle thickness. The findings suggest that nettle cultivation on marginal lands could be a viable option for producing short-fibre composites, thereby offering a sustainable use of these otherwise underutilised areas.

Keywords: natural fibre, short fibre reinforced composite, PLA, compounding, injection moulding, mechanical characterisation

1 Introduction

Since medieval times, the stinging nettle *Urtica diocia* L. has been a perennial crop used as a food, medicinal and fibre plant. The plant's low fertiliser and pesticide requirement and ability to adapt to a wide range of environmental conditions make nettle fibres an attractive option for helping to meet the growing demand for natural fibres as renewable raw materials (**Viotti et al., 2022**).

Gustav Bredemann, a German researcher, began studying and selectively cultivating wild nettles at the beginning of the 20th century. In more than 30 years of research (1918-1950), he selected the most efficient clones from 170 provenances for breeding. In addition to fibre content, his criteria included frost tolerance and growth form. As a result of these efforts, the fibre content increased from 5 % in wild nettle plants up to 17 % of stem dry matter in the cultivated species (**Bredemann, 1959**).

The combination of environmental benefits, good mechanical properties, and favourable morphological properties positions nettle fibres as a compelling alternative as a raw material for composite materials across various industries, in addition to their use in clothing textiles (**Vogl and Hartl, 2003; Harwood and Edom, 2012; Suryawan et al., 2017**). The diameter of nettle fibres ranges between 20 and 48 µm (**Jeannin et al., 2020** & **di Virgilio, 2013**). The mechanical properties of the fibres show a large scattering, which is common for natural fibres (**Bourmaud et al., 2018**). In **Jeannin et al. (2020)**, a mean Young's modulus, strain at failure and tensile strength of 54 GPa, 2.62 % and 1314 MPa were measured, while the values in **Lanzilao et al. (2016)** were 79 GPa, 2.8 % and 2196 MPa respectively. The fibre bundle tensile strength was measured as 343 ± 49 MPa (**Fischer et al. 2012**). In summary, it can be concluded that the mechanical properties are comparable to those of flax (**Jeannin et al., 2020**). Following **Bacci et al. (2010)**, the selection of the retting method affects both the morphological and mechanical properties, as well as the chemical composition of the fibres. For example, microbiological retting resulted in a cellulose content of 84.4 %, while after water retting, the cellulose proportion was 78.4 %.

Besides the fibre's interesting morphological and mechanical properties, there are economic and ecological reasons for cultivating the nettle as a fibre crop (**Viotti et al., 2022**). It is a perennial crop with low requirements in fertiliser and pesticide, and soils rich in nitrates and phosphates due to overfertilisation can be improved (**Dreyer & Müssig, 2000**). Further, the adaptability to a wide range of environmental conditions enables cultivation in various regions to easily develop regional value-added chains (**Vogl and Hartl, 2003**). Additionally, a single nettle planting can be cultivated and utilised for 10 - 15 years, which means significantly less agronomic effort like yearly field preparation and sowing compared to other fibre crops like hemp or flax, as well as a possibly lower emission of greenhouse gases due to fewer cultivation steps (**Dreyer et al., 2002**).

Another benefit of utilising stinging nettle as a fibre crop lies in its potential to thrive in contaminated soils unsuitable for food cultivation. In a study by **Jeannin et al. (2020)**, nettle crops were grown in soils containing high levels of trace elements (TE) such as mercury (Hg), arsenic (As), cadmium (Cd), lead (Pb), and zinc (Zn). The analysis revealed TE concentrations in the nettle's tissues remained far below critical levels for agronomic crops. These findings indicate that utilising soils contaminated with TE presents a viable option to increase the production of purpose-grown biomass materials while simultaneously addressing the land-use conflict arising from competing needs for food and the growing demand for plant-based fibre raw materials (**Jeannin et al., 2020)**.

The valorisation of nettle fibres from marginal lands within an agro-forestry system could address the growing need for plant-based alternatives to industrial fibres in apparel and technical products against land scarcity and the conflict between food and non-food crop production. The common nettle (*Urtica dioica* L.), with its long history as a fibre source and unique properties like high strength and length, presents an underutilised opportunity. Its suitability for cultivation on marginal or contaminated lands, where it can improve soil functionality and contribute to phyto-management, offers ecological and economic benefits. This approach not only aids in decontaminating soils but also supports wildlife habitats. Despite the composite industry's increasing demand for plant fibres, the limited availability and high cost of nettle fibres have so far hindered their widespread use. To overcome these challenges, a comprehensive strategy promoting nettle biomass utilisation on marginal lands within a sustainable agroforestry framework is proposed. The potential of nettle fibres to replace traditional fibres in biobased composites and the feasibility of developing and marketing new nettle-based materials are critical focal points.

This study aims to comprehensively analyse different nettle clones with different plant ages at harvesting time to determine their potential for reinforcing polylactide (PLA) composites for injection moulding applications. The key research questions are as follows: Can the complete nettle plant stem be directly utilised in material applications to maximise resource efficiency? What differences and measurable effects do the various separation steps have on the quality and performance of the compounds obtained?

In addition, the study will investigate the potential of using previously unused material flows from separation processes to minimise the amount of waste. Furthermore, the reinforcement effect of fibre bundles from two different mechanical separation methods, a laboratory breaking unit and a hammer mill, will be investigated and compared. These investigations are critical for understanding the performance of nettle fibre-reinforced PLA composites and provide insights into optimising processing techniques to improve the mechanical properties required for injection moulding applications. These investigations aim to answer whether nettle fibres cultivated on marginal and contaminated lands can be a sustainable replacement for traditional fibres in biobased composites and how their market viability can be enhanced.

2 Material & Methods

Composites with different raw materials from the nettle plant stem and polylactide (PLA) were produced and characterised. The goal was to evaluate the potential use of nettle fibres from different clones and separation techniques for composites.

2.1 Nettle plants and harvest

Stinging nettle stems of Roville clone were harvested one year after planting in Doncières, France (GPS coordinates: 48.389648, 6.628416). Additionally, B13 clones were harvested in Potsdam, Germany (GPS coordinates: 52.439722, 13.016306) in the same year of planting (establishing year). Stems of L18 clone were provided as baled straw from a third-party professional growing site (Frielingen, Germany, GPS coordinates: 52.980917, 9.702167) with the assistance of former NFC Nettle Fibre Company GmbH (Mölln/Groß-Helle, Germany), nowadays Felde Fibres GmbH (Dabergotz, Germany). B13 is one of the clones of an earlier breeding generation (**Bredemann, 1959**), while L18 is considered as a newer clone generation (**Fischer et al., 2019**).

2.2 Production of composites

Composite granules from seven different nettle materials and a PLA matrix were produced by compounding at 3N in Werlte, Germany. 30 mass% of each reinforcing material was compounded with 70 mass% of PLA 3251 D after drying both for 24 h at 80 °C. Details on the compounding concept are found in **Müssig et al. (2020)**.

Whole stems of the three different nettle clones, B13, Roville and L18, were cut into segments with a length of 5 cm using scissors. Without any further separation of fibrous from non-fibrous stem parts, these raw materials were compounded with the polymer for the first three composites without further separation. In addition, dew-retted stems of the L18 clone were processed using a decortication machine for fibre plant straw according to an impact principle (prototype, self-build by ATB, further labelled as hammer mill; see **Müssig et al. (2024)** for detailed information on the decortication concept).

The resulting fibre-shive mixture and the undersieve fraction, mainly containing shives, short fibres/fibre bundles and dust, were used for compounding. Due to its low content of fibre bundles, the undersieve fraction is usually not used for technical purposes and is considered a reject. By manually sorting fibres and shives, a fibre bundle content of 16.25 mass% was measured in this side stream. The main material stream of the fibre-shive mixture (fibre bundle content: 58.02 mass%) was cleaned manually by removing the shives by hand. The resulting pure fibre bundles were also compounded with PLA. A further batch of dew-retted L18 stems were decorticated with a laboratory-scale breaking unit (built by Worthmann Maschinenbau GmbH, Barßel, Germany). Each stem was passed through the breaking unit three times, with the thicker end first. The outcome was manually cleaned from shives and used for compounding. Figure 1 and Table 1 give an overview of the different nettle materials used for compounding the seven composites and the associated labels. The appearance and qualitative composition of the raw materials can be seen in Figure 1 and Figure 3. All raw materials were cut to a length of 5 to 10 cm before processing.

Table 1: Overview of reinforcement materials used for compounding with PLA matrix.

Nettle clone	Plant age at harvesting	Nettle material	Composite label
B13	Establishing year	Whole plant stem segments	B13 stems
Roville	1^{st} year	Whole plant stem segments	R stems
L18	2^{nd} year	Whole plant stem segments	L18 stems
L18	2^{nd} year	Undersieve fraction from hammer mill	L18 HM UF
L18	2^{nd} year	Fibre-shive-mixture from hammer mill	L18 HM FSM
L18	2^{nd} year	Cleaned fibre bundles from hammer mill	L18 HM fibres
L18	2^{nd} year	Cleaned fibre bundles from breaking unit	L18 BU fibres

Dog bone-shaped tensile test specimens from the composite granules were produced by injection moulding at NHL Stenden, Netherlands. Before processing, the granules were dried at 105 °C for at least 24 hr. The injection moulding for all granules was done using an Engel e-mac injection moulding machine (ENGEL AUSTRIA GmbH, Schwertberg, Austria). The temperatures in the screw cylinder were set to 150 °C, 165 °C and 175 °C and the temperature in the injector was set to 175 °C. A dwell pressure of 70 MPa for 25 sec and a cooling time of 30 sec were applied.

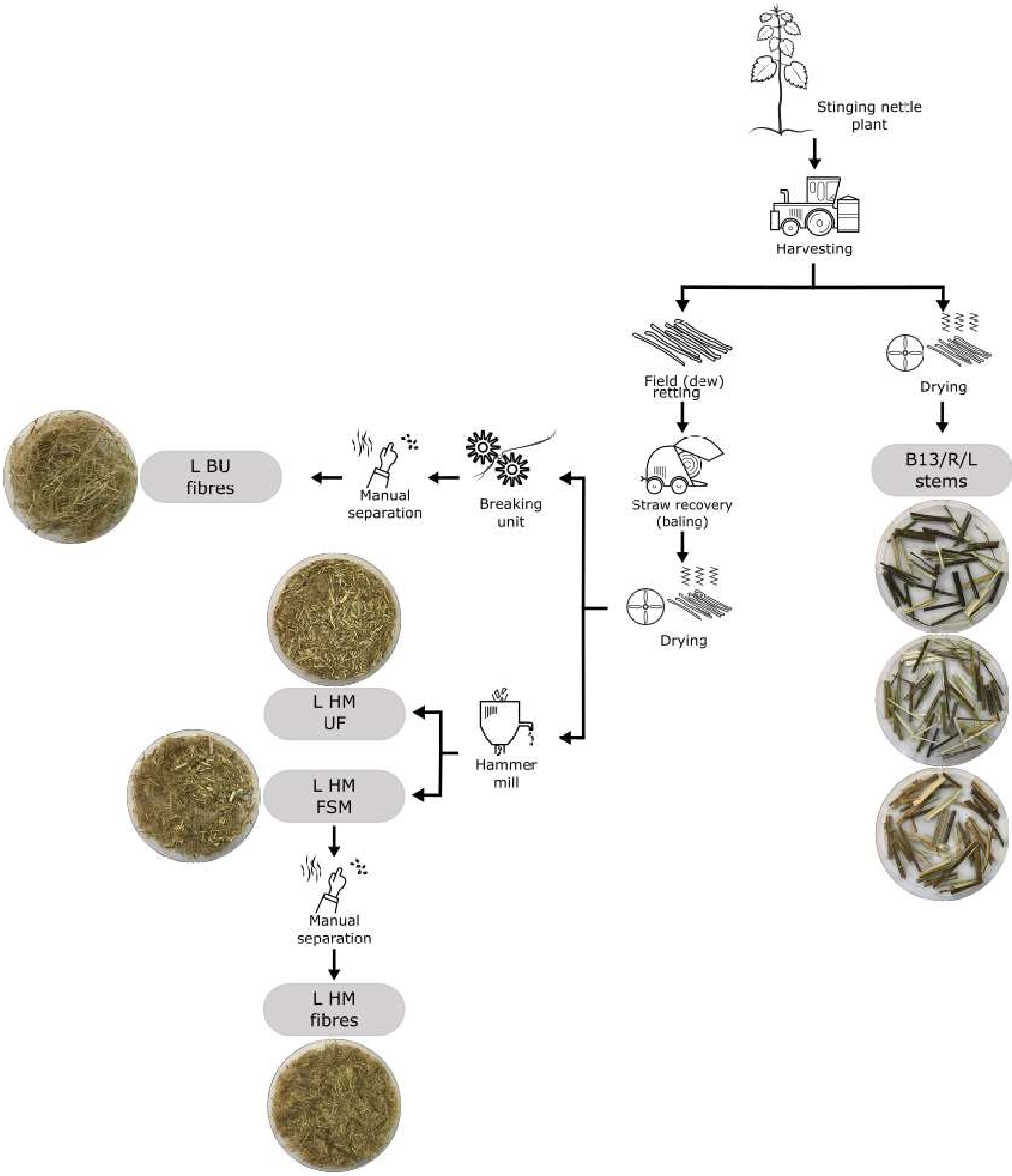

Figure 1: Processing steps of nettle plants used for compounding with the polymer matrix. All raw materials were cut to a length of 5 cm before compounding.

2.3 Mechanical characterisation of composites

Before the mechanical characterisation, the composite specimens were conditioned for 24 h at 23 °C and 50 % relative humidity according to **DIN EN ISO 291 (2008**). Tensile tests were performed following **DIN EN ISO 527-1 (1996)** and **DIN EN ISO 527-2 (1996)** using a universal testing machine type Zwick Z 020 (Zwick/Roell GmbH & Co.KG, Ulm, Germany) working with a load cell of 20 kN and a Zwick/Roell pneumatic clamping system (clamping pressure: 1.5 bar). Seven specimens per composite were pre-loaded with 50 N and then tested at a speed of 2 mm/min. Displacement for calculating Young's modulus and the strain was measured using an optical extensometer (VideoXtens, Zwick/Roell GmbH & Co. KG, Ulm, Germany).

A pendulum impact testing machine (type 5101, Zwick/Roell, Ulm, Germany) was used to determine the un-notched Charpy impact strength. Six specimens with dimensions of 80×10×4 mm^3 were tested flatwise, using a pendulum hammer of 2 J according to DIN EN ISO 179 (1997). The identical specimens were used to perform density measurements. Length, width and thickness were determined using a calliper (Mitutoyo Europe GmbH, Neuss, Germany) with an accuracy of 0.01 mm. The mass (m), determined by a scale with an accuracy of 0.01 g (type Kern 440-35n, Kern & Sohn GmbH, Balingen-Frommern, Germany) and the dimensions (V) were used to calculate the density ρ of each composite specimen using Equ. (1).

$$\rho = {}^{m}/_{V} \qquad (1)$$

2.4 Scanning electron microscopy

To further examine the structure-property relationship of the tested composites, cross-sections of plant stems of the three clones and fracture surfaces from composite specimens from impact testing were analysed using scanning electron microscopy (SEM) (JSM-6510, JEOL Ltd., Tokyo, Japan). The cross-sections were taken from dry nettle stalks, which were soaked in water for 8 hours to obtain fine cross-sections with a razor blade. After drying, the cuttings and the fracture surfaces of the composites were sputtered using a Bal-Tec sputter coater type SCD 005 (Bal-Tec, Liechtenstein) with gold for 70 s and a current of 56 mA. SEM images were made using an accelerated voltage of 5 kV.

2.5 Analyses of fibre morphology

To analyse the difference between the composites reinforced with cleaned fibre bundles from the breaking unit and the hammer mill, the fibre bundle thickness before compounding was determined using the software FibreShape (version 6.1.4, IST Innovative Scan Technologies AG, Vilters, Switzerland). For that, fibre bundle samples were cut and scanned with an EPSON Perfection V800 (SEIKO Epson CORPORATION, Japan) with a resolution of 1800 dpi. A standard measuring mask from FibreShape for measuring the bast fibre thickness with a zoom factor of 0.71 was used for object detection on these scans.

The same software was used to determine the fibre/fibre bundle thickness and length after compounding and injection moulding. The polymer matrix was dissolved using trichloromethane (≥ 99 %, Carl

Roth GmbH & Co. KG, Karlsruhe, Germany). Samples of 1 g of each composite were cut from the injection moulded specimens and put in filtering crucibles (fritted glass with porosity 3). The crucibles were filled with trichloromethane, and after 1 h, the liquid was sucked off. This procedure was repeated until the polymer was completely dissolved. The fibres were then rinsed with demineralised water, dried and spread on slide mounts and scanned with a resolution of 3400 dpi using a Reflecta ProScan 10T (Reflecta GmbH, Eutingen, Germany). The scans were analysed with FibreShape using a modified measuring mask for short fibre thickness and length. A zoom factor of 0.71 and a greyscale threshold of 240 were used to detect the fibres on the scans. The 1/Elongation-parameter in the software was changed to a minimum of 3.0.

2.6 Fibre bundle peeling test

Fibre bundle peeling tests were performed with fibre bundles from both separation methods. A schematic overview of the method used is shown in Figure 2. A total of 12 fibre bundles decorticated with the hammer mill and 10 with a breaking unit were peeled at a peeling speed of 1 µm/s over a distance of 5 mm. Details of the method can be found in **Govilas (2023)**.

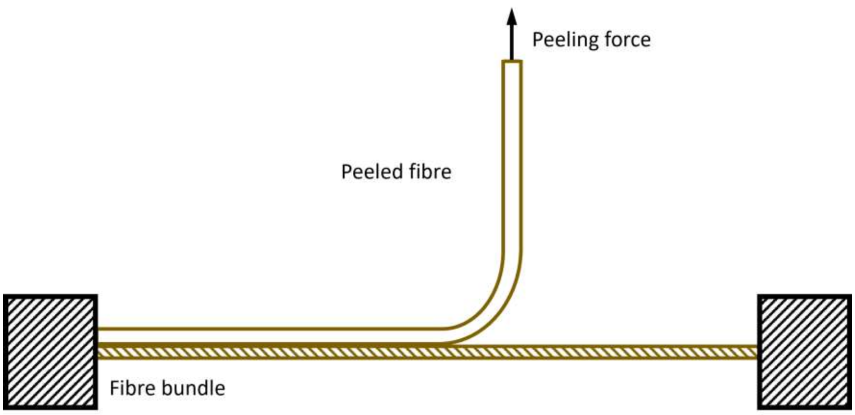

Figure 2: Schematic overview of the method to determine the decohesion force of fibre bundles (the figure is taken from **Govilas, 2013**).

2.7 Investigation of kink bands

Nettle fibre bundles from each of the two separation methods before processing the composites were prepared on slides and investigated using polarised light microscopy. Kink band regions appear lighter under polarised light due to the larger microfibril angle (MFA) (**Thygesen and Ander, 2005**). A microscope (ADL-601P, Bresser GmbH, Rhede, Germany) equipped with a digital camera (MikroCam II, 20 MP, Bresser GmbH, Rhede, Germany) was used. Kink bands were counted on three randomly selected regions of length 0.65 mm on five fibres from each separation technique. For that, RGB images were adjusted to 8-bit greyscale images. The contrast was enhanced for better visibility so the kink bands could be counted manually (see Figure 9).

2.8 Statistics

Data processing and the creation of plots were accomplished with the programming language R (version 4.3.0, https://www.r-project.org) by using built-in functions from the package ggplot2. To compare the different composite characteristics, the results were treated as follows: Firstly, a test on normal distribution using the Shapiro-Wilk test was performed ($\alpha = 0.05$). Since, for each property, at least one composite had non-normally distributed results, a one-way ANOVA on ranks (Kruskal-Wallis test, $\alpha = 0.05$) was performed to test for statistical differences. The Mann-Whitney-U test was used to test for significant differences between two composites each ($\alpha = 0.05$). Significant differences between results are marked with different letters in the plots, and non-normally distributed results are marked with an asterisk.

3 Results & Discussion

3.1 Composite processing

The production of nettle/PLA granules, followed by injection moulding of standard test specimens, was successfully realised. Figure 3 shows the different nettle raw materials, the resulting granules after compounding, and the injection moulded test specimens. It can be seen that the different nettle raw materials used for compounding led to different visual compositions within the composite. While the granules compounded with whole stem segments and the undersieve fraction contained relatively coarse particles, the cleaned fibre bundles from both the breaking unit and the hammer mill led to more homogenous granules. The composite reinforced with the fibre-shive mixture also contains coarse particles since there is still a considerable proportion of shives in the mix before cleaning. The same conclusions can be made regarding the dog bone-shaped test specimens. The SEM images (see Figure 5) confirm a homogenous distribution of the reinforcing material within the matrix polymer. Compounding different nettle materials and processing those via injection moulding produced aesthetically appealing materials based on visual control (see Figure 3).

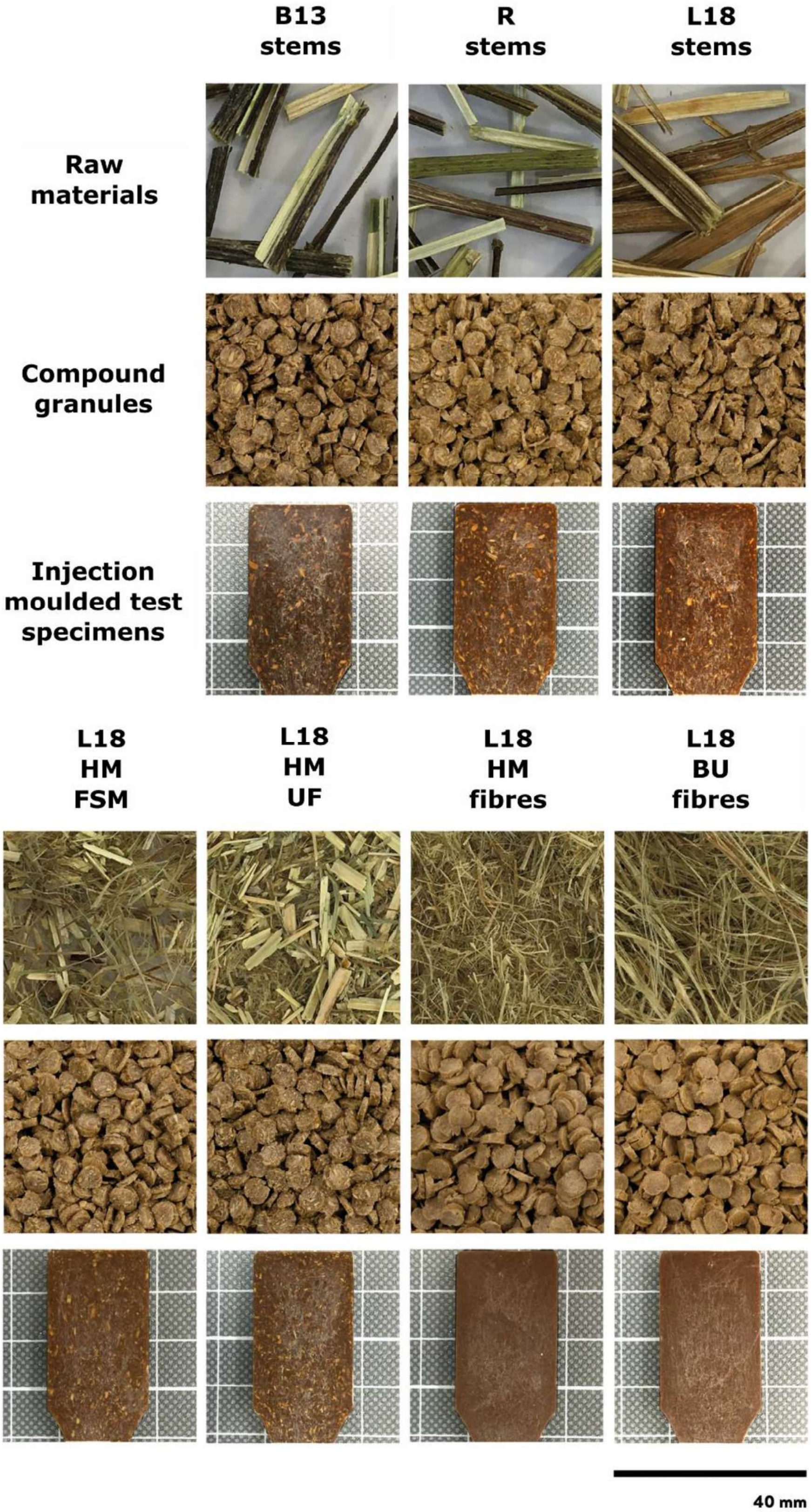

Figure 3: Overview of the seven composites with the different raw materials used as reinforcement. Row 1: raw materials; row 2: resulting composite granules; row 3: dog bone-shaped test specimens.

Table 2 shows the results from the mechanical characterisation of the composites and the pure PLA as reference. The small scattering in the density within one sample and between the different samples indicates homogeneous composite processing, thus confirming the visual findings. Adding nettle biomass generally led to a higher density than the pure PLA. The measured density value of the PLA is similar to those reported in other publications, where the same PLA type was processed via injection moulding **(Müssig et al., 2020)**. Compounding the PLA with the cleaned fibres led to the highest density values among the composites. This can be explained by the higher proportion of fibre bundles in the reinforcing material since the density of fibres was higher compared to the shives due to the shive's high degree of porosity (e.g., 76.67 % porosity for hemp shives following **Jiang et al., 2018**).

The nettle fibre bundles were shortened considerably during the compounding and injection moulding process. A mean length between 169.2 and 254.8 µm (see Table 4) was measured, comparable to the fibre lengths in compounded and injection moulded natural fibre-reinforced composites from the literature. For flax fibres, a mean length of 330 µm was found in **Le Duigou et al. (2008)** with a PLA matrix and a mean length of 191 µm in **Bos et al. (2006)** with a PP matrix. **Müssig et al. (2020)** measured a median length of 250 µm for hemp-reinforced PLA.

Table 2: Overview of the mechanical properties of all composites. Mean and standard deviation are shown for each composite and the pure PLA-matrix as a reference. The composites B13 stems, R stems, and L18 stems were compounded using whole stems of the respective nettle clones. Fractions derived from processing the L18 clone with a hammer mill include: UF (under-sieve fraction), FSM (fibre-shive mixture), and cleaned fibres. Cleaned fibres separated with a breaking unit are labelled L18 BU HM.

Composite label	Density in g/cm³	Charpy Impact strength in kJ/m²	Tensile modulus in GPa	Tensile strength in MPa	Elongation at break in %
PLA 3251 D	1.23 (± 0.01)	18.76 (± 2.17)	3.6 (± 0.1)	56.4 (± 0.3)	3.86 (± 0.32)
B13 stems	1.28 (± 0.01)	7.61 (± 0.59)	5.7 (± 0.1)	42.6 (± 1.0)	1.06 (± 0.18)
R stems	1.29 (± 0.01)	7.06 (± 0.52)	5.9 (± 0.2)	44.4 (± 0.5)	1.03 (± 0.07)
L18 stems	1.29 (± 0.01)	7.18 (± 0.61)	5.9 (± 0.2)	46.5 (± 0.5)	1.08 (± 0.04)
L18 HM UF	1.29 (± 0.01)	6.96 (± 1.25)	6.0 (± 0.2)	47.3 (± 0.3)	1.23 (± 0.19)
L18 HM FSM	1.29 (± 0.01)	8.13 (± 0.90)	6.0 (± 0.2)	50. 7 (± 0.5)	1.19 (± 0.24)
L18 HM fibres	1.30 (± 0.01)	9.24 (± 0.89)	8.1 (± 0.1)	61.8 (± 0.5)	1.20 (± 0.08)
L18 BU fibres	1.30 (± 0.01)	9.40 (± 0.37)	7.2 (± 0.3)	55.9 (± 0.4)	1.16 (± 0.23)

3.2 Tensile properties & structure-property relations

The measured mechanical properties of the pure PLA are in good agreement with data from the literature, e.g., **Müssig et al. (2020)** and **Pappu et al. (2019)**. For all nettle/PLA-composites, a significant increase in Young's modulus compared to pure PLA could be shown (see Figure 4). The tensile strength of the composites was significantly lower compared to PLA, except for the two composites reinforced with the cleaned fibre bundles (see Figure 4). This could indicate that the shives formed defects in the composite, which led to failure under a lower tensile load. This hypothesis is supported by the SEM images of the fracture surfaces (Figure 5). On the surfaces of the composites with whole plant stem segments and the fibre-shive mixture, significantly coarser particles could be identified, which could initiate cracks under tensile load and thus lead to earlier failure. Consequently, the strain at failure was significantly lower for all tested composites compared to PLA, while no difference could be shown among the different composites (see Table 2).

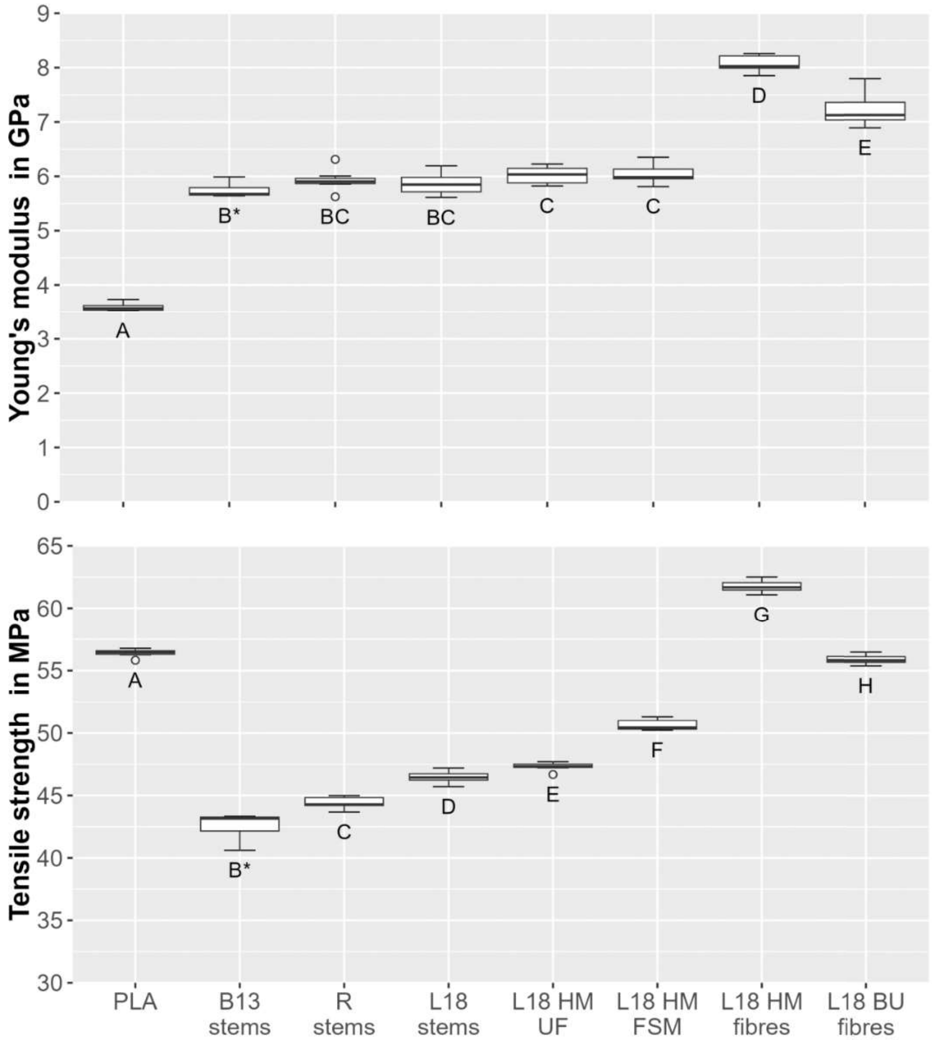

Figure 4: Box-whisker plots of Young's modulus (top) and tensile strength (bottom) of pure PLA as a reference and the PLA-nettle composites. Different letters indicate significant differences between the test samples, and asterisks mark samples that were not normally distributed.

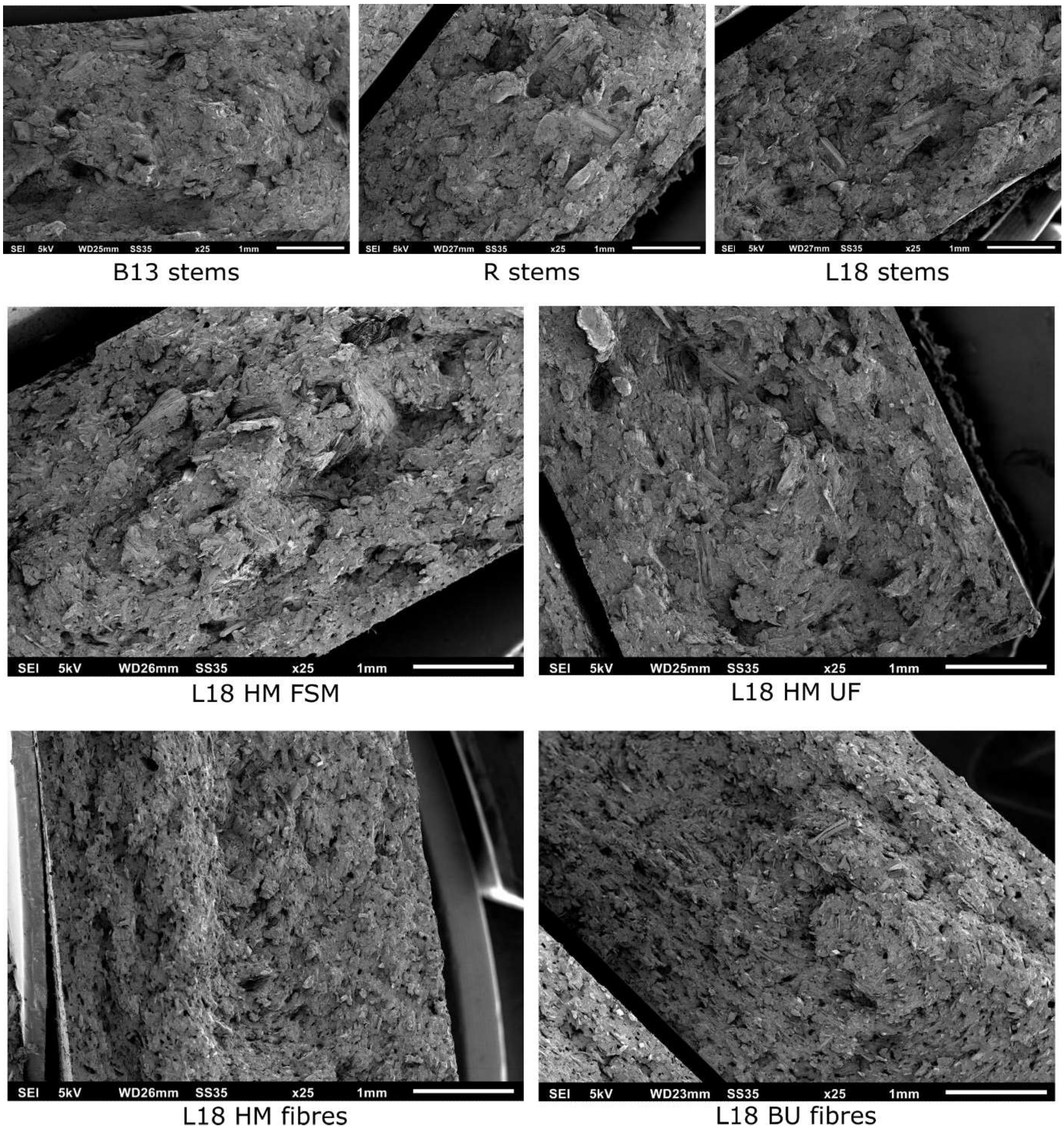

Figure 5: SEM images from the fracture surfaces of specimens from all tested composites after tensile testing. It can be seen that the compounds reinforced with the whole nettle stems contain coarse particles. Also, the compounds L18 HM FSM and L18 HM UF still contain shives, but less.

No significant differences between the composites compounded with whole stem segments from the three different nettle clones were found regarding the strain at failure and Young's modulus. In terms of tensile strength, reinforcing PLA with stems from the L18 clone led to the highest results, while using stems from the B13 clone had the lowest reinforcing effect. The results may be attributed to two factors: the age of the plants at the time of harvest and the specific purpose of breeding the different nettle clones. The B13 stems were harvested during their establishing year, while the Roville stems were cut after one year of cultivation. Typically, nettle plants intended for fibre production in the textile industry are not harvested before the second year of cultivation due to a small stem diameter and plant height, high degree of branching, and excessive leaf growth (**Bredemann, 1959**). The stems from the L18 clone were from at least two-year-old plants, resulting in a higher stem quality than the other clones following **Bredemann (1959)**. The Roville clone was cultivated as a forage plant, so the goal in breeding was a high number of leaves. The clones B13 and L18 were bred to achieve a high fibre content and quality. In Figure 6, SEM images of the stems of the three clones are shown, illustrating the distribution and compactness of bast fibres within the bast layer of the stem. The bast fibres, prominently located at the outer periphery of the stem cross-section, appeared more densely packed and had a higher content in the L18 and B13 clones than the Roville clone. Fibres in the stem of the B13 clone seem to have a larger lumen, indicating the fibres are not fully developed when harvest is done in the same year of planting. This could explain the low tensile properties at the fibre level and, therefore, the lowest tensile strength of the compound reinforced with the stems of the B13 clone. Additionally, the fibres of this clone showed the lowest aspect ratio after extracting from the tensile bars (4.79, see Table 4). Despite this being a qualitative assessment, the SEM images support the hypothesis that the L18 clone exhibited a higher bast fibre content due to its plant age at harvesting, potentially contributing to its higher tensile strength.

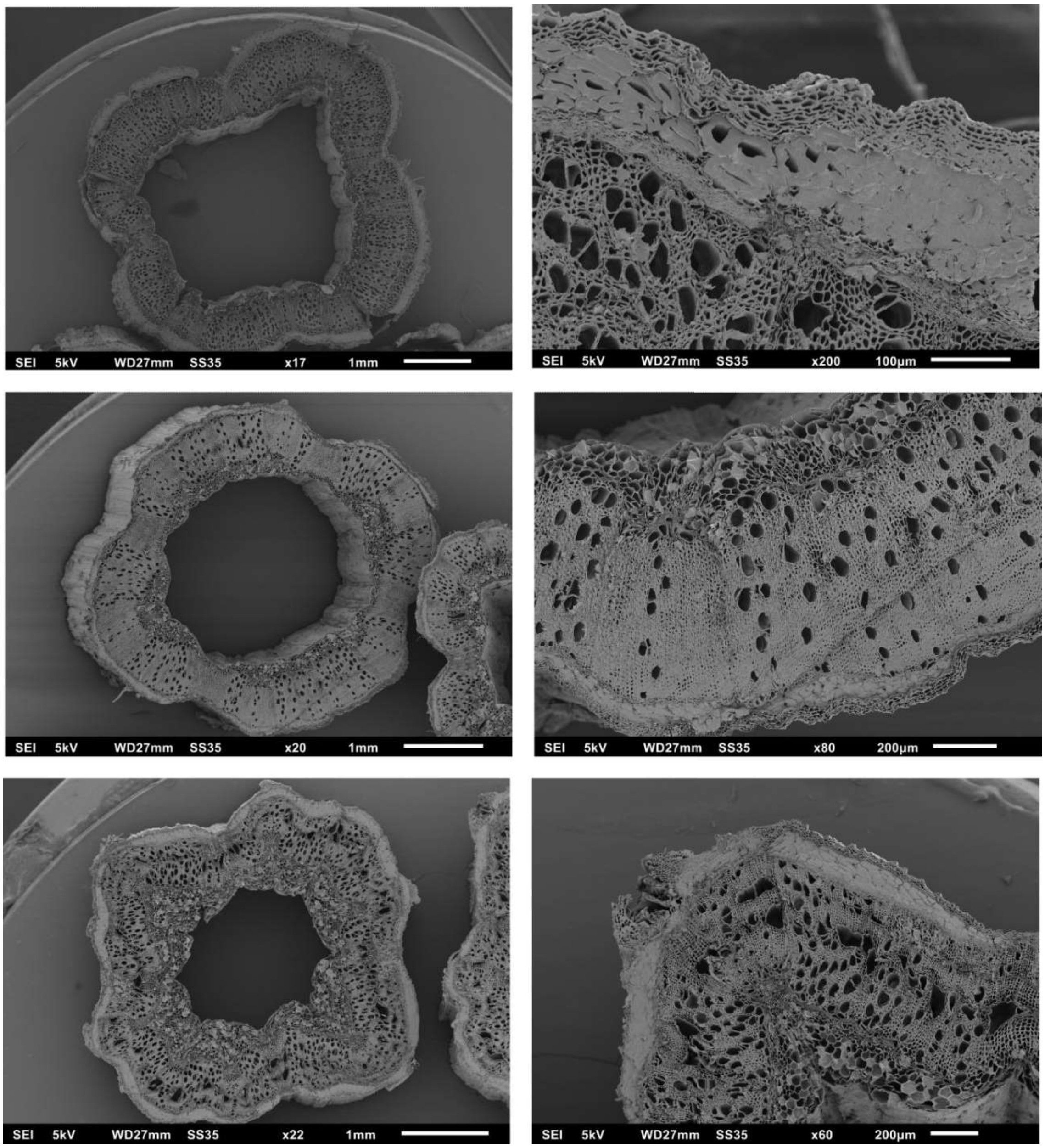

Figure 6: SEM images of stem cross-sections from nettle clones B13 (top), Roville (middle) and L18 (bottom). The bast fibres are located within the bast tissue layer at the periphery of the stem.

Processing stems from the L18 nettle clone with the hammer mill produced a fibre-shive mixture and an undersieve fraction, the latter being mostly shives and considered a reject. In this study, four composite materials were made using different forms of the L18 clone, including whole stem segments, the undersieve fraction, the fibre-shive mixture, and manually cleaned fibre bundles. All four compounds showed significantly higher Young's moduli and lower strain at failure compared to the pure polymer (see Figure 4 and Table 2). No statistical difference was shown between the compounds with whole stem segments, the undersieve fraction and the fibre-shive mixture. Reinforcing the PLA with cleaned fibre bundles led to the highest Young's modulus. The same can be concluded for the tensile strength, while using the whole stem segments led to the lowest tensile strength. The values for the composite containing undersieve fraction and the fibre-shive mixture lay in between, with all differences being statistically significant (see Figure 4). Overall, the cleaned fibre bundles showed the best reinforcing effect. These results can be explained by the different fibre content in the reinforcing materials. While the fibres have high tensile properties (e.g., fibre bundle tensile strength: 343 ± 49 MPa; single fibre Young's modulus: 26,451 ± 14,445 MPa in **Fischer et al., 2012**), shives and dust tend to cause voids/defects in the compound, which lower the mechanical performance. In addition, differences in the aspect ratio could explain the different tensile strengths. The aspect ratio of natural fibres is a critical property in composite materials because it directly influences the mechanical properties, such as tensile strength, by enhancing stress transfer between the fibre and matrix. A higher aspect ratio generally leads to improved reinforcement efficiency, resulting in stronger and more durable composite structures. Table 4 shows that the aspect ratio of fibres in the compounds L18 stems and L18 HM UF is the lowest, followed by L18 HM FSM and, with L18 HM fibres having the highest value.

An analytical model was applied to further investigate the differences in tensile strength between these four compounds. Since the application of the classical rule of mixture (ROM, see Eq. (2)) usually leads to an overestimation of the composite tensile strength in short-fibre reinforced composites, a modified rule of mixture (mROM, see Eq. (3)) was applied.

$$\sigma_C = V_f \sigma_f + V_m {\sigma'}_m \tag{2}$$

$$\sigma_C = \phi_1 \phi_2 V_f \sigma_f + V_m {\sigma'}_m \tag{3}$$

V_f and V_m represent the volumetric fractions of fibre and matrix. σ_f and σ_C are the tensile strengths of fibre and composite. For the matrix, the tensile stress at the average compound failure strain (1,2 %) ${\sigma'}_m$ (rounded to 43 MPa) was applied in the equation. Following the Cox shear lag model (**Cox, 1952**), ϕ_1 represents a filler orientation distribution factor. This factor can be expressed using the filler orientation limit angle α_0 (**Krenchel, 1964**) by Eq. (4). The Cox model assumes that the interface can effectively transfer shear stress, with both the fibre and matrix responding elastically and no axial force being transmitted through the fibre ends.

$$\phi_1 = cos^4(\alpha_0) \tag{4}$$

α_0 would be considered 1 for oriented fibres and 1/5 for fillers with random orientation (**Zhao et al., 2020**). In the Cox shear lag model, ϕ_2 represents a filler length distribution factor, which is given by Eq. (5).

$$\phi_2 = 1 + \frac{\tanh(\beta s)}{\beta s} \tag{5}$$

Here, s is the aspect ratio of fillers (see Table 4), while β denotes a shear parameter. This parameter represents the coefficient of stress concentration rate at the end of the fillers and is represented by Eq. (6).

$$\beta = \sqrt{\frac{2\mathrm{E_m}}{\mathrm{E_f}(1 + \nu_\mathrm{m})\ln(1/\mathrm{V_f})}} \tag{6}$$

with ν_m as the Poisson's ratio of the matrix (PLA: ν_m = 0.33) and $\mathrm{E_f}$ & $\mathrm{E_m}$ being the Young's modulus of fibres and matrix. This length distribution factor ϕ_2 takes values between 0 and 1 and takes a value close to 1 for a continuous fibre in 0 ° direction (**Zhao et al., 2020**).

For the calculation of the theoretical tensile strength, the actual fibre volume fraction V_{fa} was calculated and then used. Since all compounds were produced with a filler mass fraction of 30 mass%, a filler volume fraction $\mathrm{V_f}$ of 25,88 % was calculated using the density of the matrix (ρ = 1.23 g/cm³) and the fibres (ρ = 1.51 g/cm³, value taken from **Yu and Franck, 2005**). Given the varying fibre content in the reinforcing materials, the actual fibre volume fraction, V_{fa}, was calculated accordingly (see Table 3). This calculation accounted for the specific fibre content of each material, ensuring an accurate representation of the fibre distribution within the final composite structures.

The results of the analytical models are shown in Table 3, together with the experimental results. The application of the ROM led to a substantial overestimation of the tensile strength for the compounds with higher actual fibre fraction (L18 HM FSM & L18 HM fibres). Applying the mROM for these compounds, results that closely align with the experimental findings were found. The compounds with lower actual fibre content (L18 HM stems & L18 HM UF) were underestimated by the mROM while the ROM results align with the experimental findings. This indicates, that filler length and orientation are of less importance for compounds with lower fibre content. Thus, the hypothesis that the increasing fibre content, together with an increasing aspect ratio, contributes to the measured values can be considered confirmed via the analytical approach.

Table 3: Tensile strength values (in MPa) calculated by applying the classical rule of mixture (Eq. (2)) and the modified rule of mixture using the Cox shear lag model (Eq. (3)). Also shown are the experimental values in comparison.

Compound	**Fibre mass fraction in the compounded biomass in %***	**Actual fibre volume fraction in the composite V_{fa} in %**	**Tensile strength - calculated: ROM**	**Tensile strength - calculated: mROM**	**Tensile strength – experimental (mean)**

L18 HM stems	11.00	2.85	41.6	33.2	46.5
L18 HM UF	16.25	4.21	46.3	34.0	47.3
L18 HM FSM	58.02	15.02	83.4	44.5	50.7
L18 HM fibres	100.00	25.88	120.6	59.4	61.8

** The nettle fibre content in the compounded nettle biomass (100 % means pure fibres; 0 % means biomass without any fibre)*

Comparing the tensile properties of compounds reinforced with cleaned nettle fibres separated by two different methods reveals that fibres processed with the hammer mill provide a superior reinforcing effect. This resulted in significantly higher tensile strength and Young's modulus. To clarify this difference, two hypotheses were investigated:

1) Fibre bundles and fibres from separation via hammer mill had a lower thickness and a higher aspect ratio (length/thickness).
2) Separation of fibre bundles and fibres using the breaking unit led to more defects and kink bands in the nettle fibres, lowering their tensile properties on the single fibre level.

In an initial approach, the morphological properties of the fibre bundles after separation (before compounding) were measured via FibreShape. The fibre bundles generated by the hammer mill showed significantly lower thickness values. The same can be concluded for the fibres after chemical extraction from the injection moulded specimens (see Figure 7). However, a higher aspect ratio was found in the fibres separated using the breaking unit (Table 4). This is because those fibre bundles showed not only a larger fibre bundle thickness but also a greater length compared to the bundles from separation with the hammer mill.

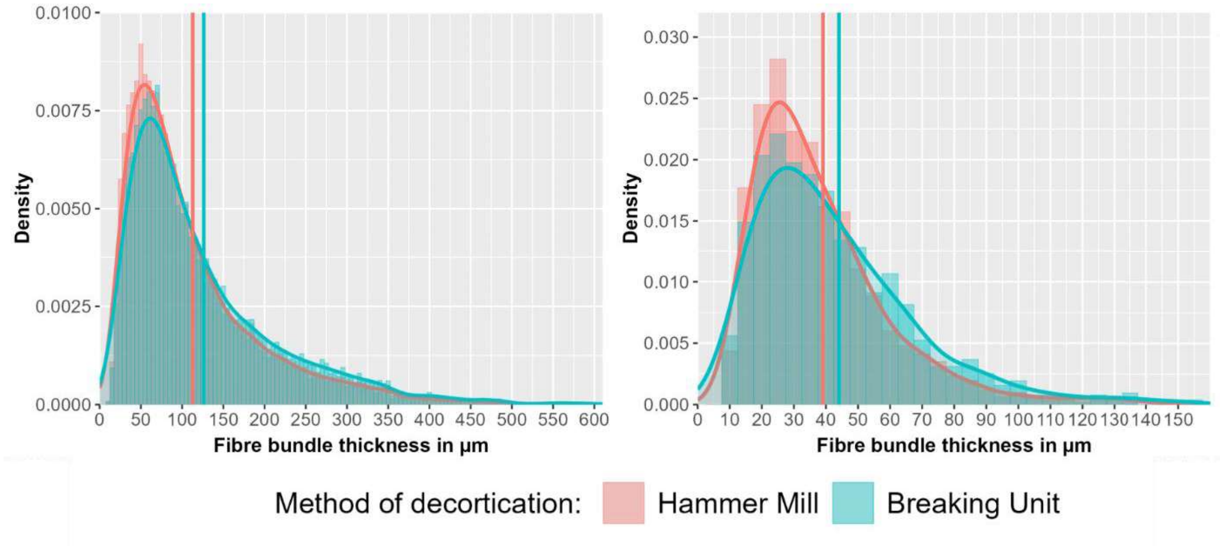

Figure 7: Density histograms with kernel density estimation curve (bin width = 5 µm) of the thickness of cleaned nettle fibre bundles from separation via breaking unit and hammer mill before processing (left) and after extraction from the injection moulded specimen (right). The means are shown as vertical lines in the respective colour, and a statistically significant difference between the bundles from the two decortication methods could be proven in both cases.

Table 4: Thickness, length and aspect ratio of the reinforcing materials after extraction from injection moulded specimens.

Compound	Thickness in µm	Length in µm	Aspect ratio: length/thickness
B13 stems	38.74	191.67	4.79
R stems	33.36	169.17	5.19
L18 stems	42.82	206.95	4.89
L18 HM UF	42.16	204.37	4.72
L18 HM FSM	47.34	254.84	5.15
L18 HM fibres	39.10	208.20	5.23
L18 BU fibres	44.07	249.07	5.75

These differences might be intriguing because one would expect similar morphological properties for the same type of natural fibre after compounding and injection moulding with the same processing parameters. This expectation arises from the fact that compounding with a twin-screw extruder followed by injection moulding is generally considered a detrimental process for natural fibres, leading to a strong size reduction in the transverse (decohesion) and the longitudinal (fragmentation) direction of the fibre bundles. This is due to the high shear rate generated during the processes and the transmission of shear forces to the fibre bundles. The degree of size reduction is influenced by various parameters, including the screw speed and the flow rate (**Beaugrand and Berzin, 2013**). In **Berzin et al. (2017)**, the average fibre length and diameter of hemp in a polypropylene matrix were measured along the length of a twin-screw extruder. The object length was decreased from initially 12 mm to around 1.75 mm, and the diameter from 250 µm to around 68 µm.

A plausible explanation for the greater length and thickness of the fibre bundles after separation with the breaking unit combines both the reduced cohesiveness of the fibre bundles and the different principles of decortication. After separation using the hammer mill, the fibre bundles exhibit reduced cohesiveness, possibly due to changes or degradation of the middle lamella during processing, which facilitates easier separation and results in thinner bundles or even individual fibres. Furthermore, the hammer mill operates on an impact-based principle, subjecting the stalks to random, disorderly stress, which leads to a higher degree of cross-cutting and transverse size reduction. In contrast, the breaking unit applies pressure and low shear along the fibre orientation as the plant stalks are stressed between the crusher rollers, preserving the fibres' longitudinal structure. This combined effect of lower cohesiveness and different processing principles explains the formation of thinner fibre bundles in the composite reinforced with hammer mill-separated fibres.

To investigate the hypothesis of changes in the middle lamella, fibre bundle peeling tests were performed. This method allows the determination of the decohesion force required to separate a single fibre from a fibre bundle. An interfacial adhesion energy per unit of area is calculated for each case as the ratio of the peeling force to the apparent peeled single-fibre diameter. In most cases, the peeling force did not exceed 10 mN. Figure 8 shows the results of a tested fibre. The force data, plotted as a function of the peeling distance, exhibits gradual increases punctuated by abrupt drops. These increases are associated with regions along the fibre interface that present greater resistance to decohesion. A lower average adhesion energy within the fibre bundles after separation by the hammer mill (0.22 ± 0.10 mN/µm) compared to the separation with the breaking unit (0.27 ± 0.14 mN/µm) was shown. Fibre bundles separated using a hammer mill appeared easier to separate, indicating a higher degree of single-fibre individualisation within the bundles (**Akleh et al., 2023**).

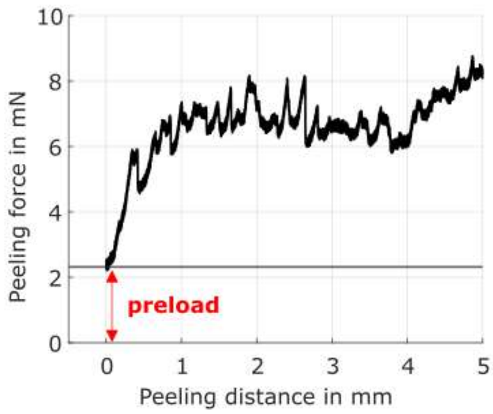

Figure 8: Peeling test result of a nettle fibre; the peeling force is shown as a function of the peeling distance (Akleh et al., 2023).

The number of kink bands per length was examined to investigate the hypothesis of different degrees of fibre damage due to the two different separation techniques. In kink band regions, the cellulose orientation deviates from defect-free regions, which can influence the mechanical behaviour of fibres (**Grégoire et al., 2020**). Different separation methods and parameters might affect the number of kink bands and, therefore, the mechanical properties. The relationship between the fibre separation method, the occurrence of kink bands, and the mechanical characteristics was studied for flax fibres in **Morgillo et al. (2023)**. The highest number of kink bands was found for the most intensively combed batch of flax (18.2 kink bands/mm).

For nettle fibres, **Davies and Bruce (1998)** found a correlation between the degree of damage of the fibre, quantified by the kink band area, and the fibre's Young's modulus and tensile strength. The more kink bands were found, the lower tensile properties were measured. **Andersons et al. (2009)** reported a correlation between the tensile strength and kink bands in flax fibres.

A mean of 47.07 kink bands per mm was counted for the fibres separated with the breaking unit, while for fibres from the hammer mill, it was a mean of 25.77 kink bands per mm. This trend supports the hypothesis that separating the fibres with the breaking unit led to higher damage to the fibres. These findings can also be connected to the fibre bundle peeling tests. The smaller diameters and greater ease of separability observed in fibres processed by the hammer mill support the hypothesis that hammer mill separation results in less fibre damage compared to separation using roller breakers for the processed nettle stems. Since kink band regions were not always clearly distinguishable from the defect-free regions on the microscope images, it is important to state that these numbers were more of a qualitative approach showing a trend that might explain the measured compound properties.

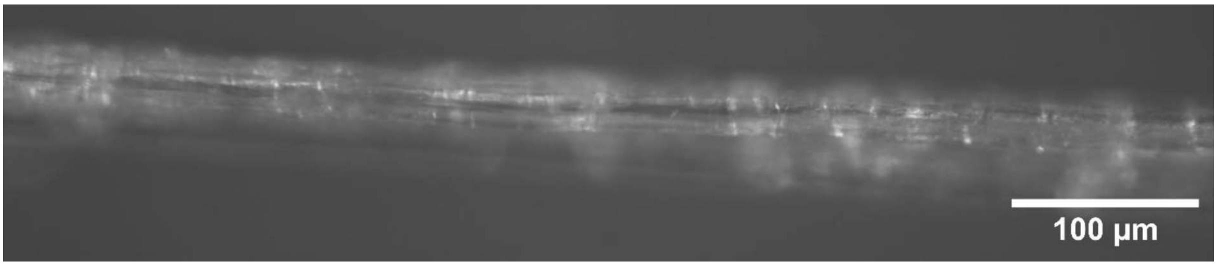

Figure 9: Visualisation of kink bands on a fibre bundle after separation with the breaking unit using polarised light microscopy.

In conclusion, while both hypotheses provided valuable insights into the observed differences in the mechanical properties of the two compounds reinforced with cleaned nettle fibre bundles, neither fully accounted for the results. The actual behaviour of the compounds was likely influenced by a combination of factors addressed in each hypothesis. Therefore, further investigation, e.g., synchrotron micro-CT to examine the kink band regions in more detail, is required to fully understand the underlying mechanisms and to accurately attribute the observed differences to specific factors or a potential interplay between them (Richely et al., 2023). Additionally, further explanations might account for the differences which may involve variations in surface properties of the particles, such as differences in wetting behaviour and surface energy.

3.3 Impact properties

Overall, the mean Charpy impact strength of all composites was significantly lower (range: 6.96 kJ/m² to 9.4 kJ/m²) compared to the pure polymer (18.76 kJ/m²). This matches the expectation of a lower impact strength when reinforcing a polymer with stiff bast fibres. This also has been measured for nettle-reinforced PLA in **Fischer et al. (2012)**, where the un-notched Charpy impact strength also dropped by more than 50 % from 24 kJ/m² for the pure PLA to 11 kJ/m² when reinforcing it with 30 mass% of nettle fibres via compression moulding.

Among the tested composites, the two composites with cleaned fibre bundles as reinforcement showed the highest impact strength, while the lowest values were found when compounding the PLA with the undersieve fraction from the hammer mill and the whole stem segments (see Figure 10). No statistically significant difference between the composites reinforced with the whole stem segments, the undersieve fraction or the fibre shive mixture was found. This could be explained by the higher total fibre volume fraction within the cleaned fibre bundles, leading to more energy dissipation through fibre pull-out. The SEM images (see Figure 5) show a higher number of pulled-out fibre ends at the fracture planes of the composites with cleaned fibre bundles as raw material. From the two compounds with cleaned fibre bundles, the separation with the breaking unit led to slightly higher values. This difference can be explained by the greater fibre bundle length in the compound compared to separation with the hammer mill (see Table 4), leading to a higher degree of fibre pull-out under impact load.

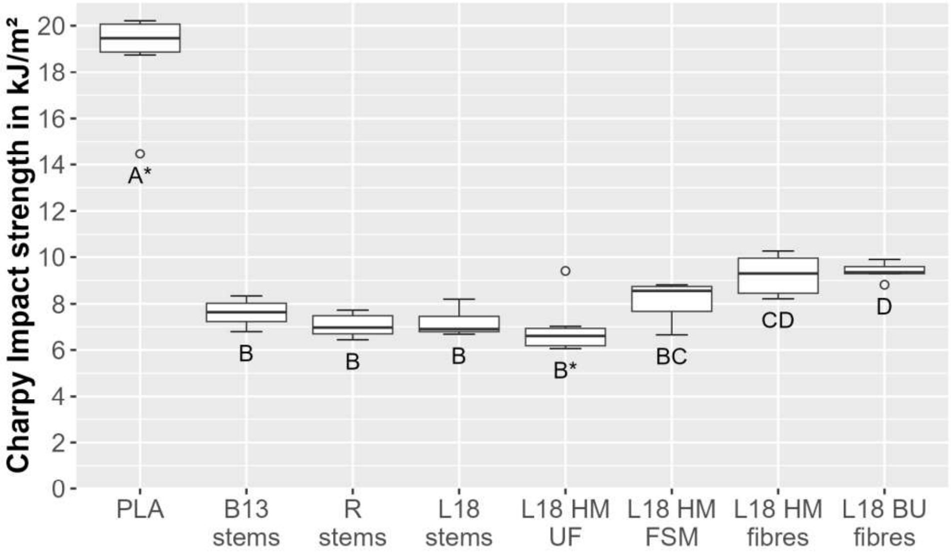

Figure 10: Box-whisker plot of the un-notched Charpy impact strength of the pure PLA, as a reference, and the PLA-nettle composites. Different letters indicate significant differences between the samples, and asterisks mark samples that were not normally distributed. Outliers are shown as circles.

Adding an impact modifier during the compounding process can improve the impact properties of bast fibre-reinforced polymers. For example, in **Mat Taib et al. (2014)**, an ethylene acrylate copolymer impact modifier was successfully applied to improve the impact properties of a kenaf/PLA composite.

In summary, the mechanical properties of the nettle fibre composite materials are promising. Coupled with the findings of **Jeannin et al. (2020)**, which indicate that trace element levels in nettle fibres from cultivation on contaminated soils remain well below tolerable thresholds for agronomic use, it can be concluded that cultivating biomass on trace-element-contaminated soils presents a viable strategy. Additionally, in **Viotti et al. (2024)**, nettle could be grown on Hg-contaminated soils. The study demonstrated the potential to increase crop yield and fibre production per plant while reducing Hg concentration in the leaves using organic amendments. The approach of nettle cultivation on marginal lands increases the supply of purpose-grown fibre materials while also helping to alleviate land-use conflicts between food production and the growing demand for plant-based fibre resources.

4 Conclusions

- Seven reinforcement materials were produced from the three stinging nettle clones B13 (establishing year), Roville (1st year) and L18 (established plant; >2nd year). The reinforcements were as follows:
    - B13 clone whole plant stem segments,
    - Roville clone whole plant stem segments,
    - L18 clone whole plant stem segments,
    - L18 clone undersieve fraction from hammer mill,
    - L18 clone uncleaned fibre-shive mixture from hammer mill,
    - L18 clone cleaned fibre bundles from hammer mill,
    - L18 clone cleaned fibre bundles from breaking unit.
- All seven nettle materials were successfully compounded with PLA as a matrix (30 mass% of biomass and 70 mass% of polymer).
- The produced granules were successfully processed by injection moulding, leading to aesthetically pleasing materials of homogenous quality.
- The Charpy impact strength of the tested composites dropped around 50 % compared to the pure PLA, as expected when adding stiff bast fibres to a polymer like PLA. The cleaned fibre bundles from both separation techniques, the breaking unit and hammer mill, led to the highest impact strengths among the tested composites. Compared to literature data on bast/PLA or hemp/PLA composites, the impact properties are at the same level.
- All the tested composites exhibited a significantly higher Young's modulus than the unreinforced PLA. Even the reinforcement of the PLA with the undersieve fraction from the hammer mill, which is usually not used for technical applications, led to a significant increase in the modulus. The tensile strength of all composites was lower than that of the unreinforced PLA, except for the two composites, which were reinforced with manually cleaned fibre bundles. Thus, rejecting the shives from the fibres significantly affects the composites' mechanical properties.
- The composite reinforced with the fibre bundles from the hammer mill had higher tensile strength and Young's modulus than those reinforced with the fibre bundles from breaking-unit separation. Possible explanations are finer fibre bundles and fewer defects caused by the hammer mill.
- The whole nettle stems, without any separation, could be successfully compounded with PLA. These composites exhibited interesting properties, e.g., Young's modulus comparable to the

composite reinforced with the fibre-shive mixture from the hammer mill. Due to the significantly lower production effort, compounding the whole stem segments with a polymer could be a promising concept for non-structural applications with a focus on high resource efficiency.

Declaration of interests

The authors declare no competing financial interests or personal relationships that could have influenced the work reported in this paper.

Data availability

Data will be made available on request.

Acknowledgement

These works have been supported by the European Union's Horizon 2020 research and innovation program under grant agreement No 771134. The project NETFIB was carried out under the ERA-NET Cofund SusCrop (Grant N°771134), being part of the Joint Programming Initiative on Agriculture, Food Security and Climate Change (FACCE-JPI). We gratefully acknowledge Prof. Dr. Michaela Eder (TUM School of Life Sciences, Freising, Germany) for her valuable feedback. We further thank Georg Gödecke and Hansjörg Wieland (3N Kompetenzzentrum Niedersachsen Netzwerk Nachwachsende Rohstoffe und Bioökonomie e.V.) for their support in compounding, as well as Corinne von Nordenne (NHL Stenden) for her assistance with injection moulding in sample production.

References

Akleh, W., Govilas, J., Beaugrand, J., Clévy, C. and Placet, V. (2023, June 19–21): Plant fiber interface adhesion characterization through peeling tests: Influence of pant variety, retting and extraction processes [Conference presentation]. 6th International Conference on Natural Fibers, Funchal, Madeira, Portugal.

Andersons, J., Poriķe, E., and Spārniņš, E. (2009): The effect of mechanical defects on the strength distribution of elementary flax fibres. *Composites Science and Technology*, 69(13), 2152-2157.

Bacci, L., Baronti, S. Predieri, S. and di Virgilio, N. (2009): Fiber Yield and Quality of Fiber Nettle (*Urtica dioica* L.) cultivated in Italy. *Industrial crops and products, 29*, 480–84.

Beaugrand, J., and Berzin, F. (2013): Lignocellulosic fiber reinforced composites: influence of compounding conditions on defibrization and mechanical properties. *Journal of Applied Polymer Science*, 128(2), 1227-1238.

Berzin, F., Beaugrand, J., Dobosz, S., Budtova, T., and Vergnes, B. (2017): Lignocellulosic fiber breakage in a molten polymer. Part 3. Modeling of the dimensional change of the fibers during compounding by twin screw extrusion. *Composites Part A: Applied Science and Manufacturing*, 101, 422-431.

Bos, H.L., Müssig, J. and van den Over, M.J.A. (2006): Mechanical properties of short-flax-fibre reinforced compounds. *Composites Part A. Applied Science and Manufacturing*, 37, 10, 1591-1604.

Bourmaud, A., Beaugrand, J., Shah, D. U., Placet, V., and Baley, C. (2018): Towards the design of high-performance plant fibre composites. *Progress in Materials Science*, 97, 347-408.

Bredemann, G. (1959): *Die große Brennnessel Urtica dioica L. Forschung über ihren Anbau zur Fasergewinnung*. Akademieverlag, Berlin, Germany.

Cox, H. L. (1952): The elasticity and strength of paper and other fibrous materials. *British journal of applied physics*, 3(3), 72.

Davies, G. C., and Bruce, D. M. (1998): Effect of environmental relative humidity and damage on the tensile properties of flax and nettle fibers. *Textile Research Journal*, 68(9), 623-629.

DIN EN ISO 527-1, 1996: *Bestimmung der Zugeigenschaften, Teil 1 – Allgemeine Grundsätze* (ISO 527-1:1996); German and English version EN ISO 527-1:1996.

DIN EN ISO 527-2, 1996: *Bestimmung der Zugeigenschaften, Teil 2 – Prüfbedingungen für Form- und Extrusionsmassen* (ISO 527-2:1996); German and English version EN ISO 527-2:1996.

DIN EN ISO 179-1, 2006: *Kunststoffe – Bestimmung der Charpy-Schlageigenschaften* (ISO 179-1:2006-05); German and English version EN ISO 179-1:2010.

DIN EN ISO 291, 2008: *Kunststoffe – Normalklimate für Konditionierung und Prüfung* (ISO 291-2008); German and English version EN ISO 291:2008.

Le Duigou, A., Pillin, I., Bourmaud, A., Davies, P. and Baley, C. (2008): Effect of recycling on mechanical behaviour of biocompostable flax/poly(L-lactide) composites. *Composites: Part A*, 39, 9, 1771-1478.

Dreyer, J., and Müssig, J. (2000): New horizons in natural fibre production: separation of hemp and nettle with enzymes. In *3rd International Symposium Biorohstoff Hanf and Andere Faserpflanzen. Wolfsburg, Germany* (pp. 13-16).

Dreyer, J., Müssig, J., Koschke, N., Ibenthal, W. D., and Harig, H. (2002): Comparison of enzymatically separated hemp and nettle fibre to chemically separated and steam exploded hemp fibre. *Journal of industrial hemp*, 7(1), 43-59.

Fischer, H., Werwein, E. and Graupner, N. (2012): Nettle fibre (*Urtica dioica* L.) reinforced poly(lactic acid): A first approach. *Journal of Composite Materials*, 46, 24 3077-3087.

Fischer, H., Gusovius, H., Lühr, C., Rödel, P., Schneider, C., Kreye, S., Machmüller, A., Rottmann-Meyer, M., Beckhaus, H. (2019): Schlussbericht zum Verbundvorhaben "InBeNeFa—Verbundvorhaben: Entwicklung einer Industriellen Bereitstellungskette von Brennnesseljungpflanzen bis zur Nesselfaser"; Research Report of the Faserinstitut Bremen; Faserinstitut Bremen: Bremen, Germany, 2019; 117p

Grégoire, M., Barthod-Malat, B., Labonne, L., Evon, P., De Luycker, E., and Ouagne, P. (2020): Investigation of the potential of hemp fibre straws harvested using a combine machine for the production of technical load-bearing textiles. *Industrial crops and products*, 145, 111988.

Garlotta, D. (2001): A literature review of poly(lactic acid). *Journal of Polymers and the Environment*, 9, 2, 63-84.

Govilas, J. (2023): *Plant fiber mechanical characterization with high precision micro-mechatronic means: investigation of single fiber transverse behavior and inter-fiber adhesion*. [Doctoral dissertation, Matériaux composites et construction, Université Bourgogne Franche-Comté]. NNT: 2023UBFCD007ff. tel- 04472025

Harwood, J. and Edom, G. (2012): Nettle Fibre: Its Prospects, Uses and Problems in Historical Perspective. *Textile History*, 43:1, 107-119, DOI: 10.1179/174329512X13284471321244

Hughes, M. (2012): Defects in natural fibres: their origin, characteristics and implications for natural fibre-reinforced composites, *Journal of Material Science,* 47, 599-609.

Jeannin, T., Yung, L., Evon, P., Labonne, L., Ouagne, P., Lecourt, M., Cazaux, D., Chalot, M. and Placet, V. (2020): Native stinging nettle (Urtica dioica L.) growing spontaneously under short rotation coppice for phytomanagement of trace element contaminated soils: Fibre yield, processability and quality. *Industrial Crops and Products*, 145, 111997.

Jiang, Y., Lawrence, M., Ansell, M. P., and Hussain, A. (2018): Cell wall microstructure, pore size distribution and absolute density of hemp shiv. *Royal Society Open Science*, 5(4), 171945.

Krenchel, H. (1964): Fibre reinforcement: theoretical and practical investigations of the elasticity and strength of fibre-reinforced materials. Akademisk Forlag, Kopenhagen, Denmark.

Lanzilao, G., Goswami, P., and Blackburn, R. S. (2016): Study of the morphological characteristics and physical properties of Himalayan giant nettle (*Girardinia diversifolia* L.) fibre in comparison with European nettle (*Urtica dioica* L.) fibre. *Materials Letters*, 181, 200-203.

Mat Taib, R., Hassan H.M. and Mohd Ishak, Z.A. (2014): Mechanical and Morphological Properties of Polylactic Acid/Kenaf Bast Fiber Composites Toughened with an Impact Modifier. *Polymer-Plastics Technology and Engineering*, 53:2, 199-206.

Mohanty, A. K., Vivekanandhan, S., Pin, J. and Misra, M. (2018): Composites from renewable and sustainable resources: Challenges and innovations. *Science*, 362, 6414, 536-542.

Morgillo, L., Brionne, L., Melelli, A., Ouagne, P., Scheel, M., Weitkamp, T., Shah, D.U., Abida, M., Beaugrand, J. and Bourmaud, A. (2023): Elucidating links between the mechanical performance of flax fibres and their structural defects. *Industrial Crops and Products*, 206, 117722.

Müssig, J., Haag, K., Musio, S., Bjelkove, M., Albrecht, K., Uhrlaub, B., Wang, S., Wieland, H. and Amaducci, S. (2020): Biobased ‘Mid-performance’ composites using losses from the hackling process of long hemp – A feasibility study as part of the development of a biorefinery concept – A feasibility study as part of the development. *Industrial Crops and Products*, 145, 111938.

Müssig, J., Enke, S., Gusovius, H., Lühr, C., Uhrlaub, B., Dammer, L., and Carus, M. (2024): Mechanical separation of kenaf for composite applications - Evaluation of the total fibre line concept for field retted kenaf. *Industrial Crops and Products*, 208, 117870.

Pappu, A., Pickering, K.L. and Thakur, V.K. (2019): Manufacturing and characterization of sustainable hybrid composites using sisal and hemp fibres as reinforcement of poly (lactic acid) via injection moulding. *Industrial Crops and Products*, 137, 260-269.

Richely, E., Zarei, A., Melelli, A., Rajan, D. K., Govilas, J., Gabrion, X., Clévy, C., Legland, D., Perez, J., Guessasma, S., Placet, V., Kallio, P. and Beaugrand, J. (2023). Measurement of microfibril angle in plant fibres: Comparison between X-ray diffraction, second harmonic generation and transmission ellipsometry microscopies. *Composites Part C: Open Access*, *11*, 100355.

Sawpan, M.A., Pickering and K.L., Fernyhough, A. (2007): Hemp fibre reinforced poly (lactic acid) composites. *Advanced Materials Research,* 29, 337-340.

Suryawan, A.I.G.P., Suardana, N. P. G., Suprapta Winaya, I. N., Budiarsa Suyasa, I. W., and Tirta Nindhia, T. G. (2017): Study of stinging nettle (urtica dioica l.) Fibers reinforced green composite materials: a review. *IOP conference series: materials science and engineering*, 201, 1, 012001

Thygesen, L.G. and Ander, P. (2005): Quantification of dislocations in spruce pulp and hemp fibres using polarized light microscopy and image analysis. *Nordic Pulp & Paper Research Journal,* 20, 1, 64-71.

Viotti, C., Albrecht, K., Amaducci, S., Bardos, P., Bertheau, C., Blaudez, D., Bothe, L., Cazaux, D., Ferrarini, A., Govilas, J., Gusovius, H., Jeannin, T., Lühr, C., Müssig, J., Pilla, M., Placet, V., Puschenreiter, M., Tognacchini, A., Yung, L. and Chalot, M. (2022): Nettle, a Long-Known Fiber Plant with New Perspectives. *Materials*, 15, 4288. https://doi.org/10.3390/ma15124288

Viotti, C., Bertheau, C., Martz, F., Yung, L., Placet, V., Ferrarini, A., Fornassier, F., Blaudez, D., Puschenreiter, M., and Chalot, M. (2024): Digestate Improves Stinging Nettle (Urtica dioica) Growth and Fiber Production at a Chlor-Alkali Site. *Plants*, 13(17), 2425.

di Virgilio, N. (2013): Stinging nettle: a neglected species with a high potential as multi-purpose crop. Summer school of FIBRA. National Research Council of Italy. Institut of Biometeorology. Catania, Italy.

Vogl, C.H. and Hartl, A. (2003): Production and processing of organically grown fiber nettle (*Urtica dioica* L.) and its potential use in the natural textile industry: A review. *American Journal of Alternative Agriculture*, 18, 119-128.

Yu, C. and Franck, R. R. (2005): Pineapple, curauá , craua (caroá), macambira, nettle, sunn hemp, Mauritius hemp and fique . In R. R. Franck (Edt.), Bast and other plant fibres (3rd ed., pp. 79–98). Woodhead Publishing Limited, Cambridge, England.

Zhao, S., Zhao, Z., Yang, Z., Ke, L., Kitipornchai, S., and Yang, J. (2020): Functionally graded graphene reinforced composite structures: A review. *Engineering Structures*, 210, 110339.

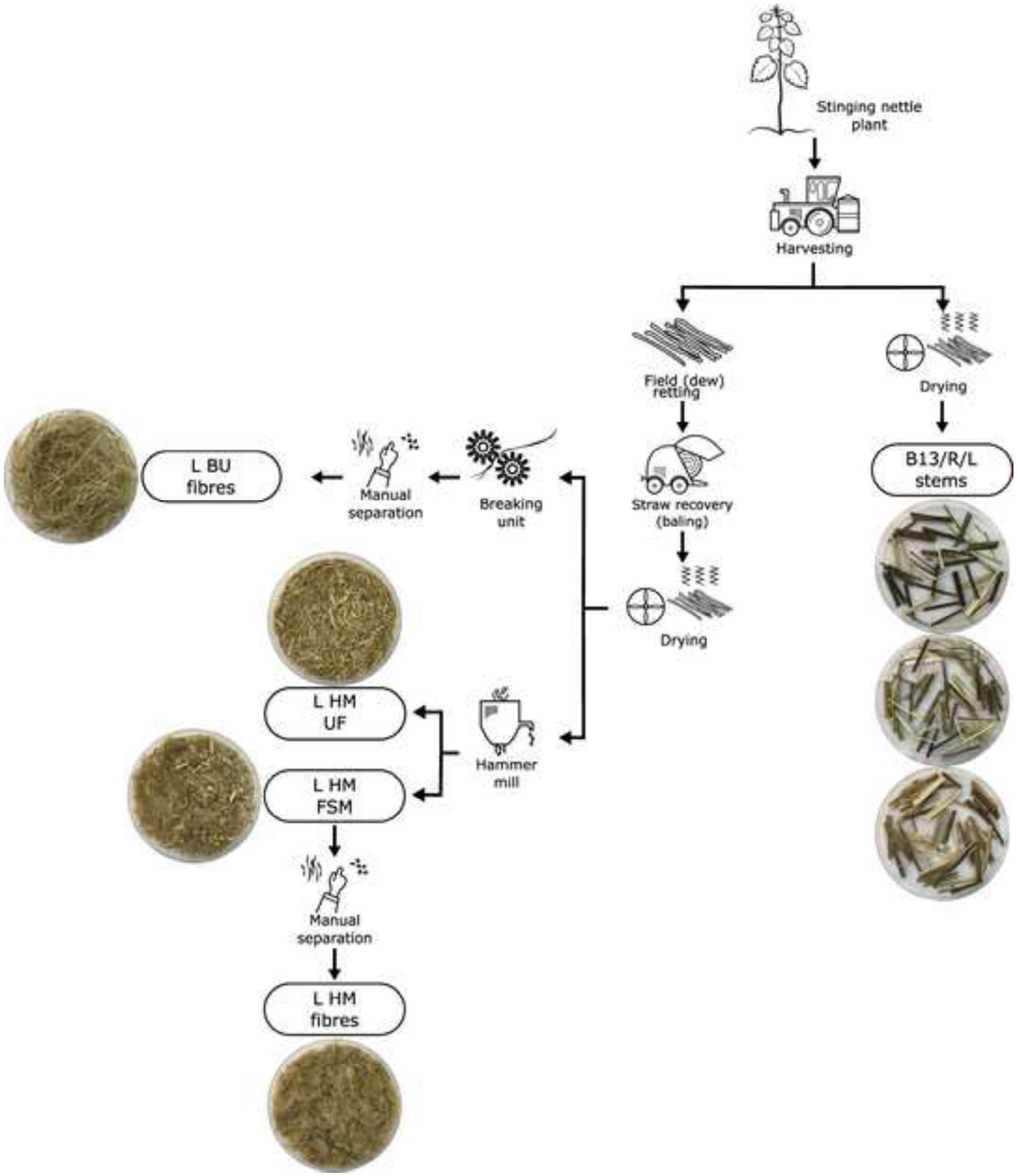
Stinging nettle plant
Harvesting
Field (dew) retting
Drying
Straw recovery (baling)
B13/R/L stems
Drying
L BU fibres
Manual separation
Breaking unit
L HM UF
L HM FSM
Hammer mill
Manual separation
L HM fibres

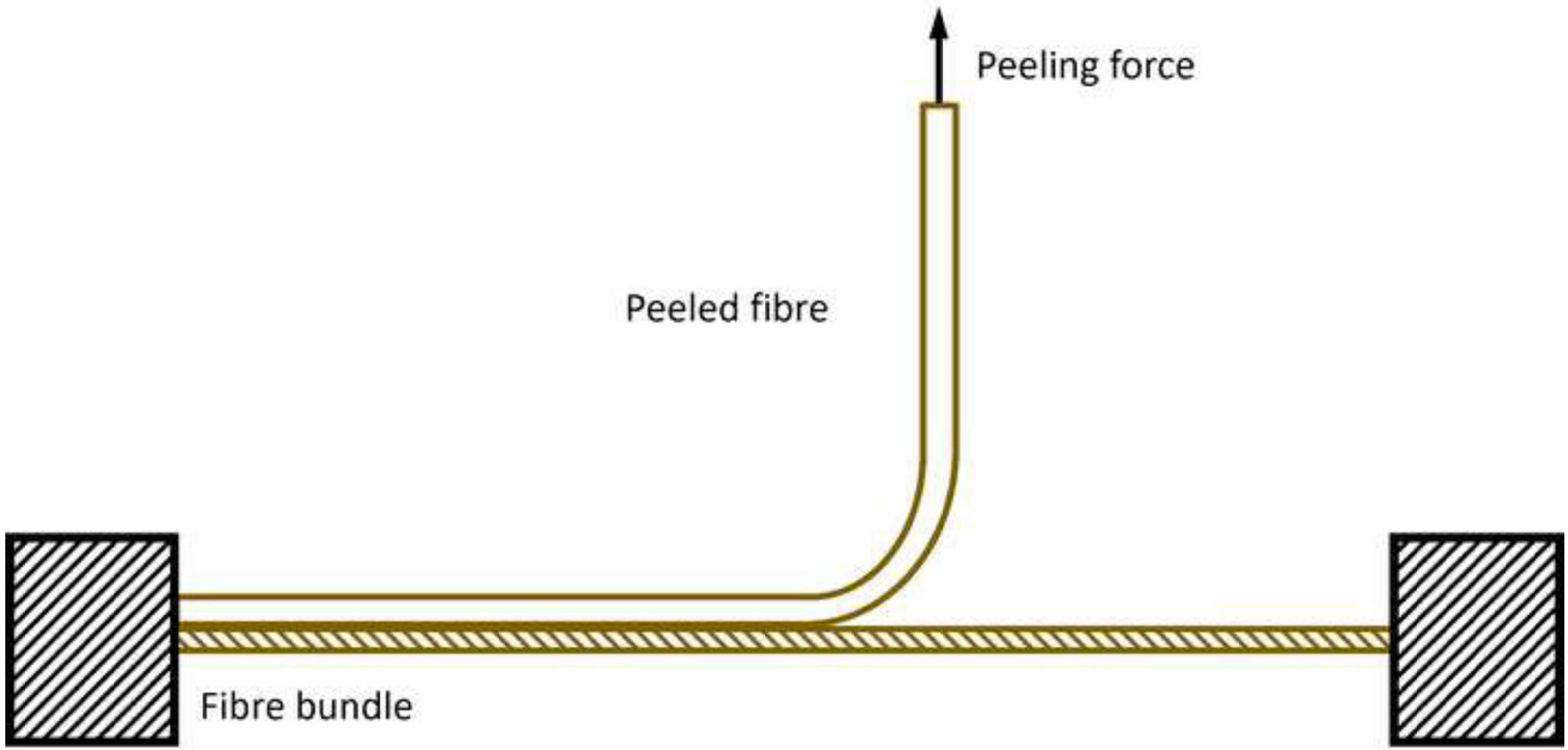
Peeling force
Peeled fibre
Fibre bundle

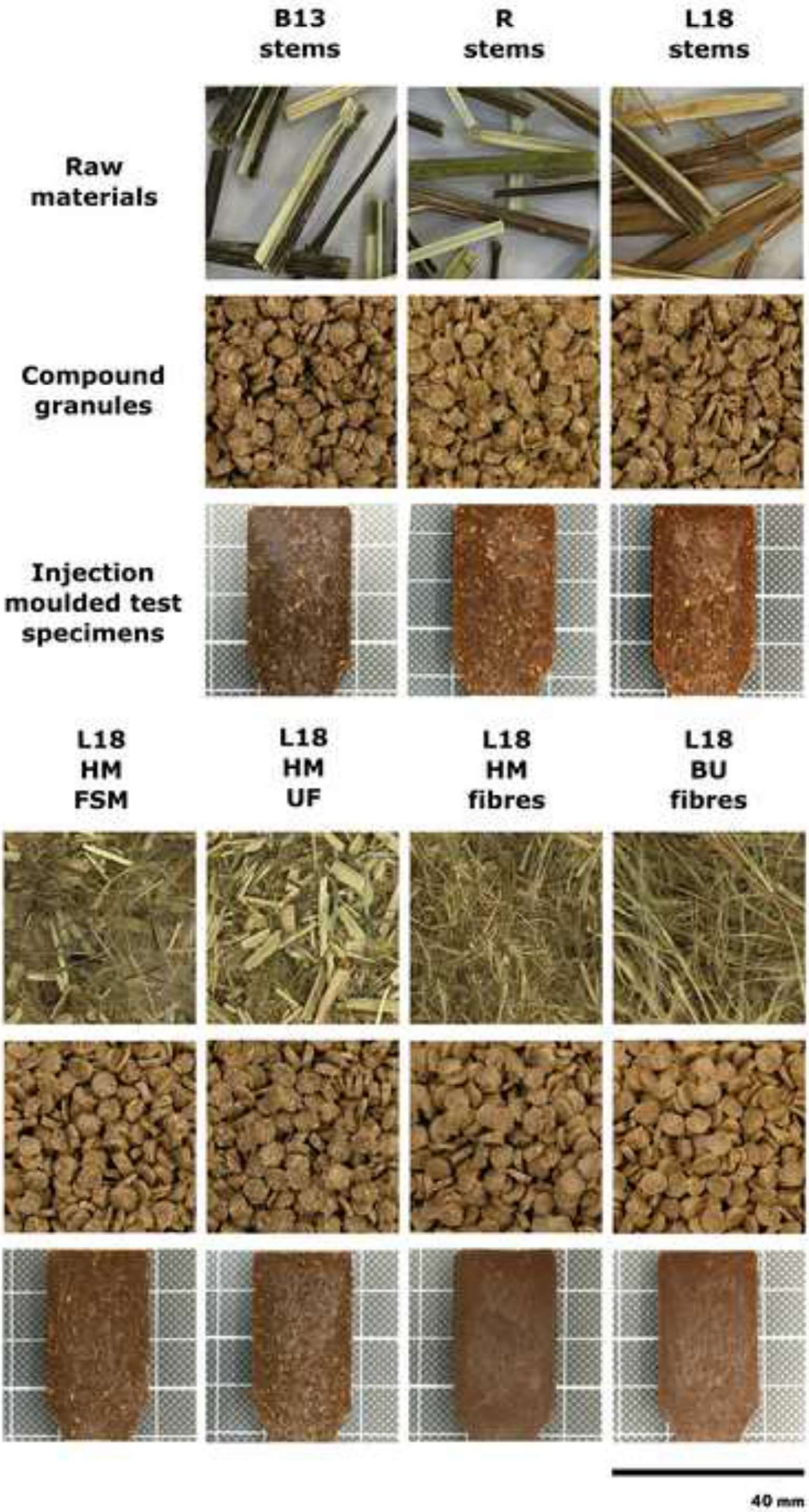
B13
stems
R
stems
L18
stems
Raw
materials
Compound
granules
Injection
moulded test
specimens
L18
HM
FSM
L18
HM
UF
L18
HM
fibres
L18
BU
fibres
40 mm

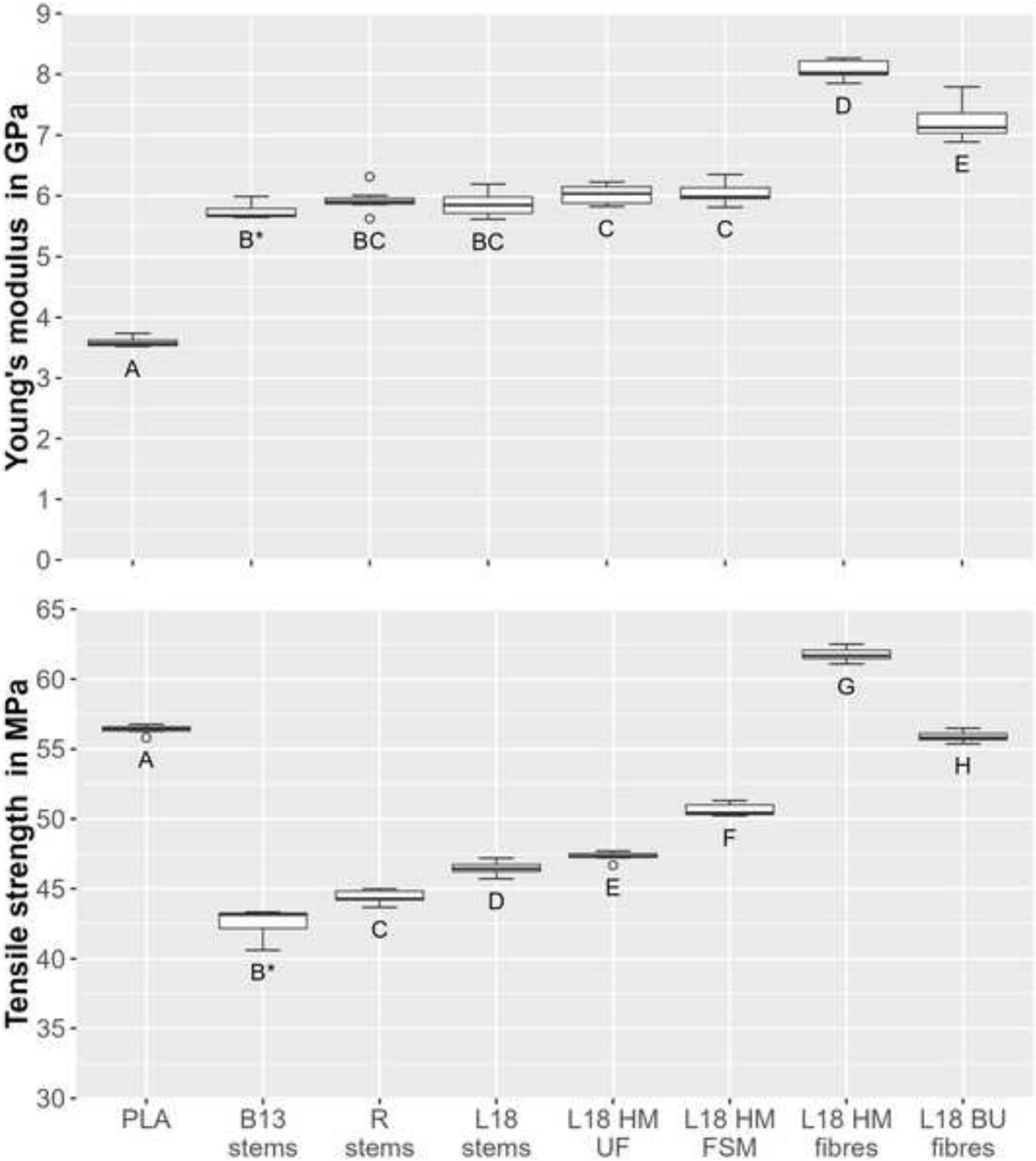

Young's modulus in GPa
0
1
2
3
4
5
6
7
8
9
A
B*
BC
BC
C
C
D
E
Tensile strength in MPa
30
35
40
45
50
55
60
65
A
B*
C
D
E
F
G
H
PLA
B13 stems
R stems
L18 stems
L18 HM UF
L18 HM FSM
L18 HM fibres
L18 BU fibres

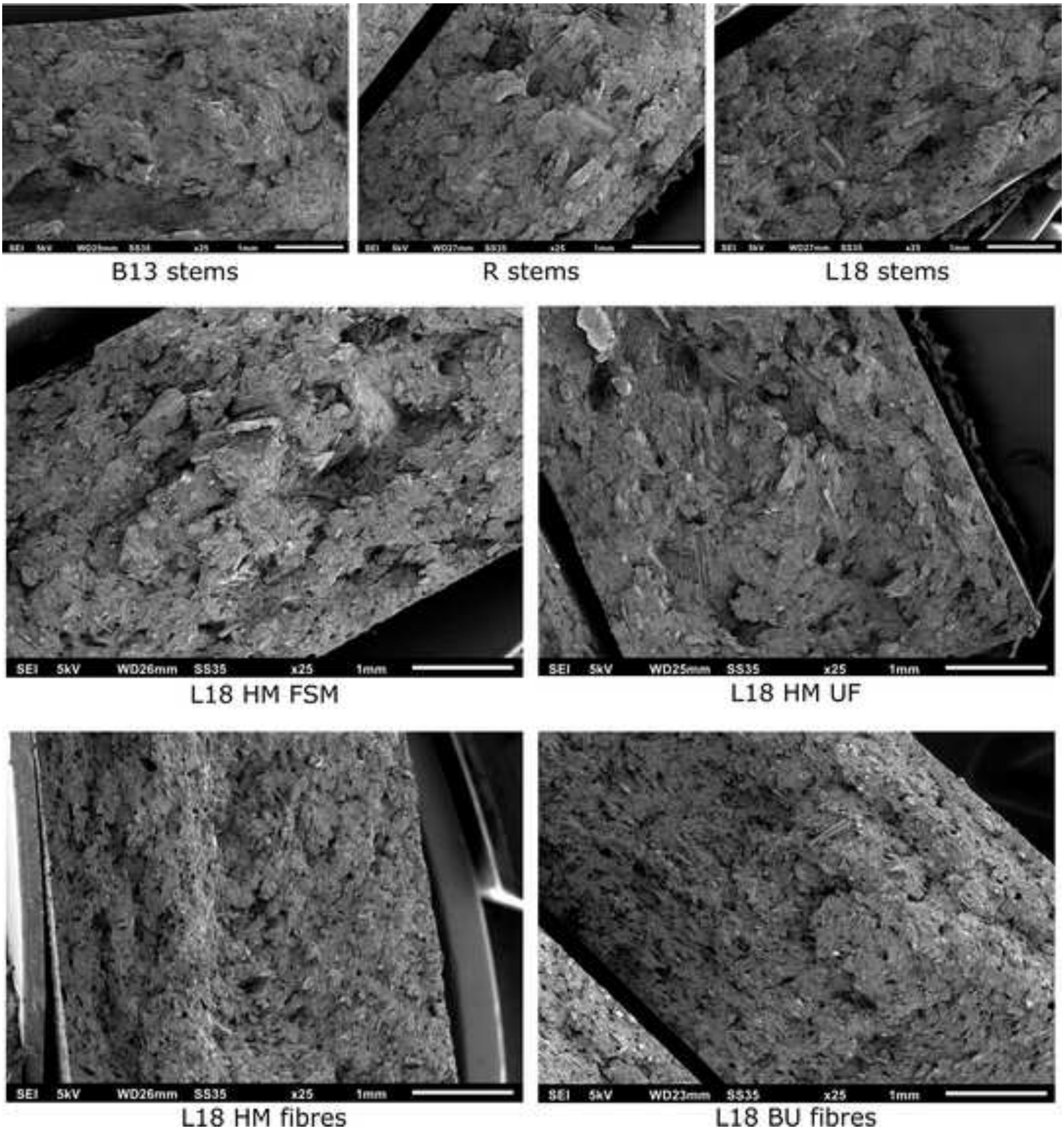
B13 stems
R stems
L18 stems
SEI 5kV WD26mm SS35 x25 1mm
L18 HM FSM
SEI 5kV WD25mm SS35 x25 1mm
L18 HM UF
SEI 5kV WD26mm SS35 x25 1mm
L18 HM fibres
SEI 5kV WD23mm SS35 x25 1mm
L18 BU fibres

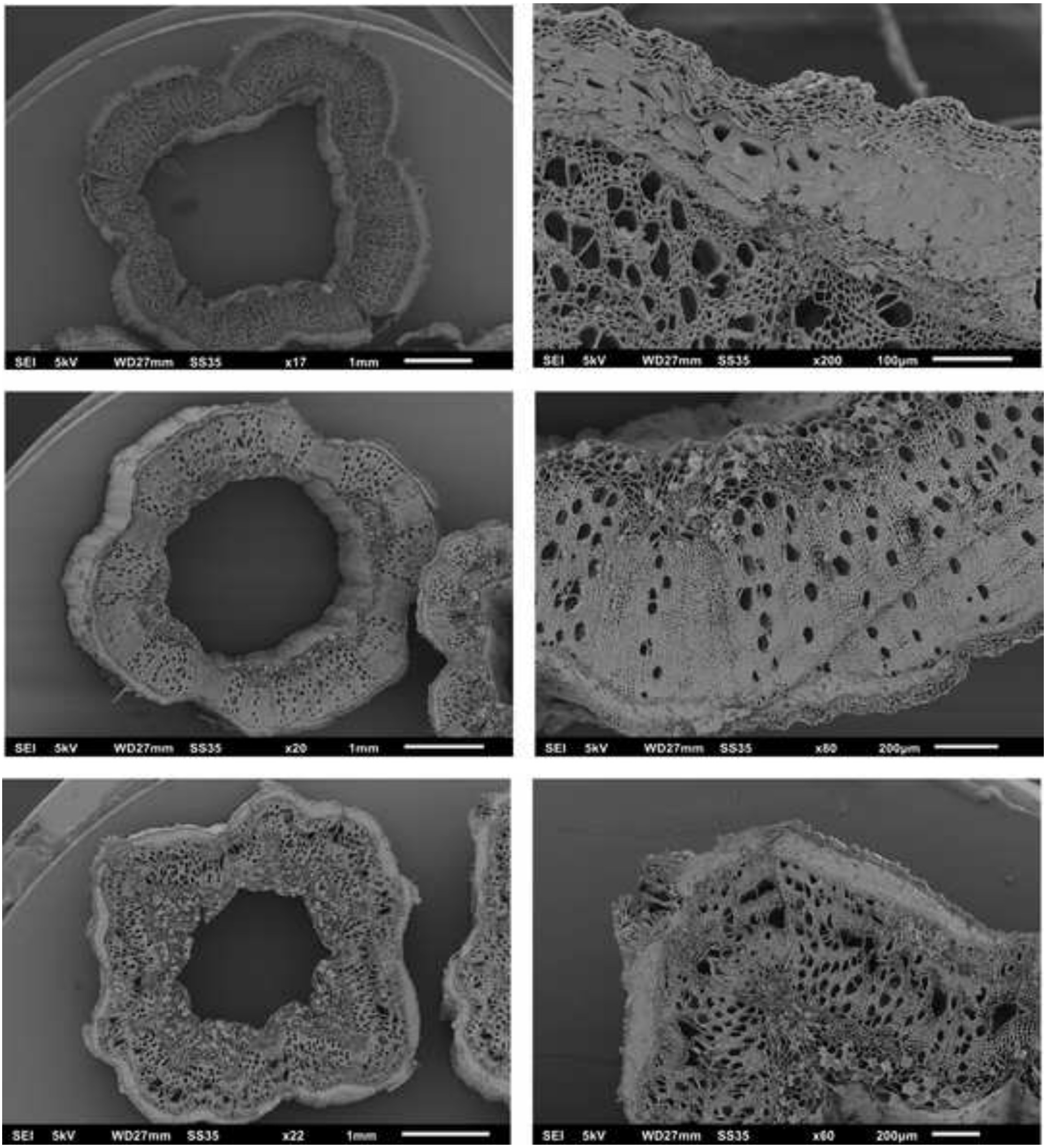
SEI 5kV WD27mm SS35 x17 1mm
SEI 5kV WD27mm SS35 x200 100µm
SEI 5kV WD27mm SS35 x20 1mm
SEI 5kV WD27mm SS35 x80 200µm
SEI 5kV WD27mm SS35 x22 1mm
SEI 5kV WD27mm SS35 x60 200µm

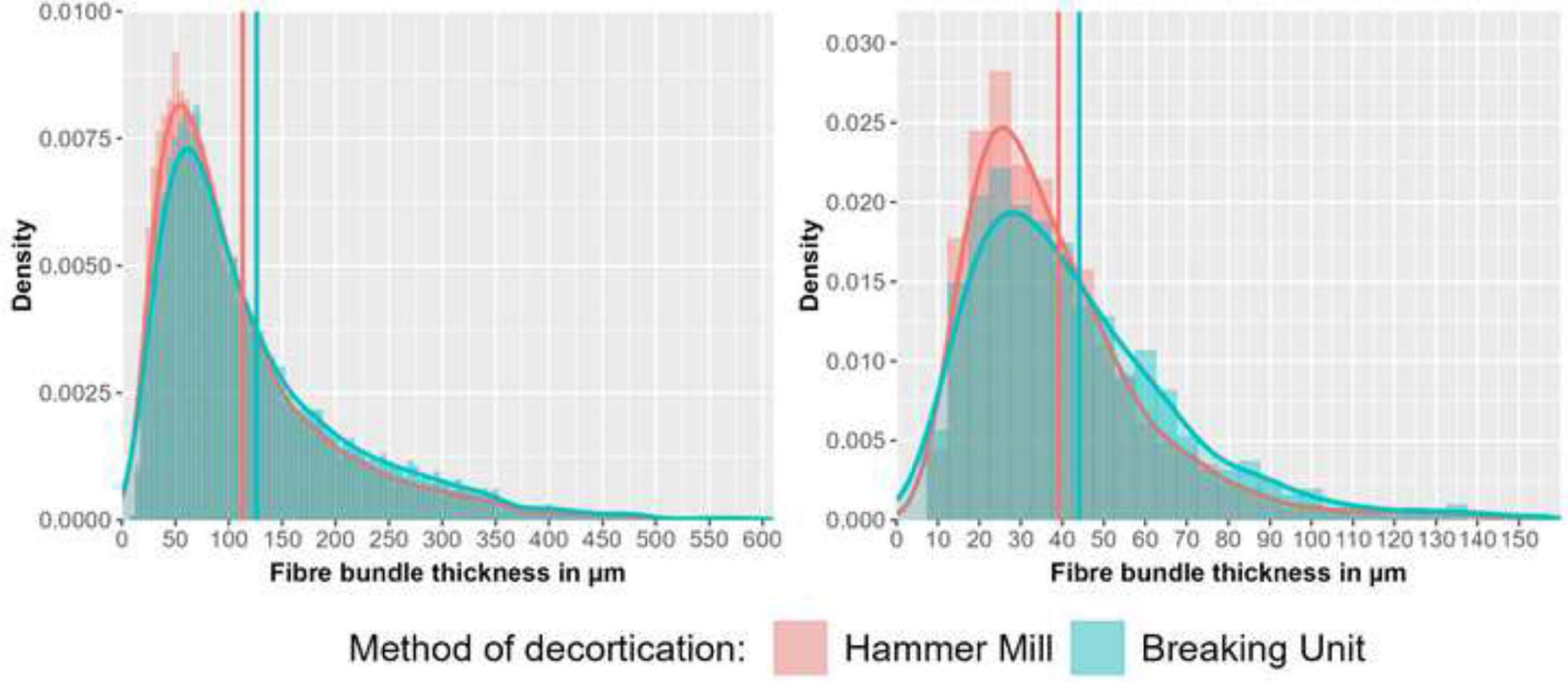

0.0100
0.0075
0.0050
0.0025
0.0000
Density
0
50
100
150
200
250
300
350
400
450
500
550
600
Fibre bundle thickness in µm
0.030
0.025
0.020
0.015
0.010
0.005
0.000
Density
0
10
20
30
40
50
60
70
80
90
100
110
120
130
140
150
Fibre bundle thickness in µm
Method of decortication:
Hammer Mill
Breaking Unit

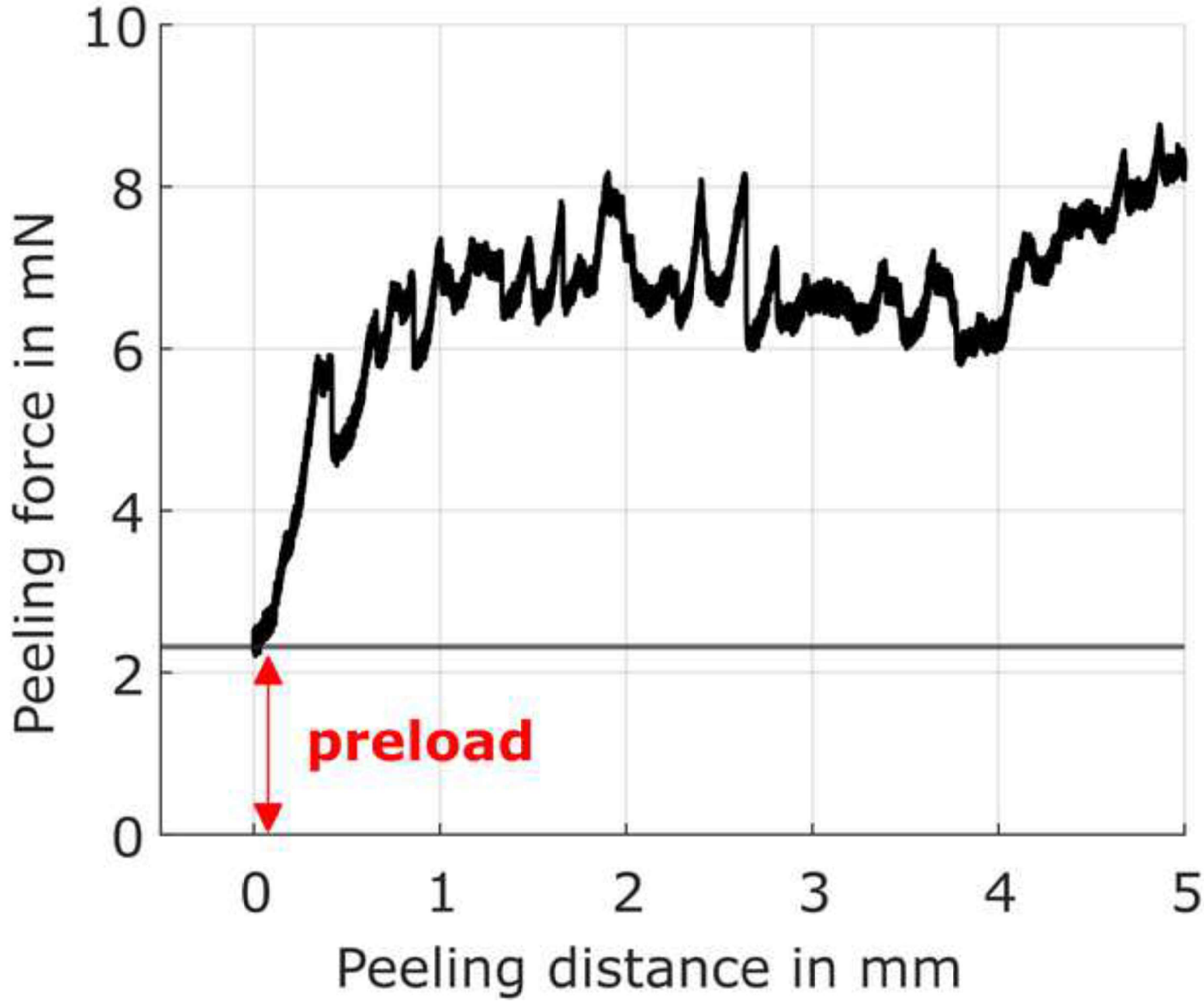
Peeling force in mN
10
8
6
4
2
0
preload
0
1
2
3
4
5
Peeling distance in mm

Figure

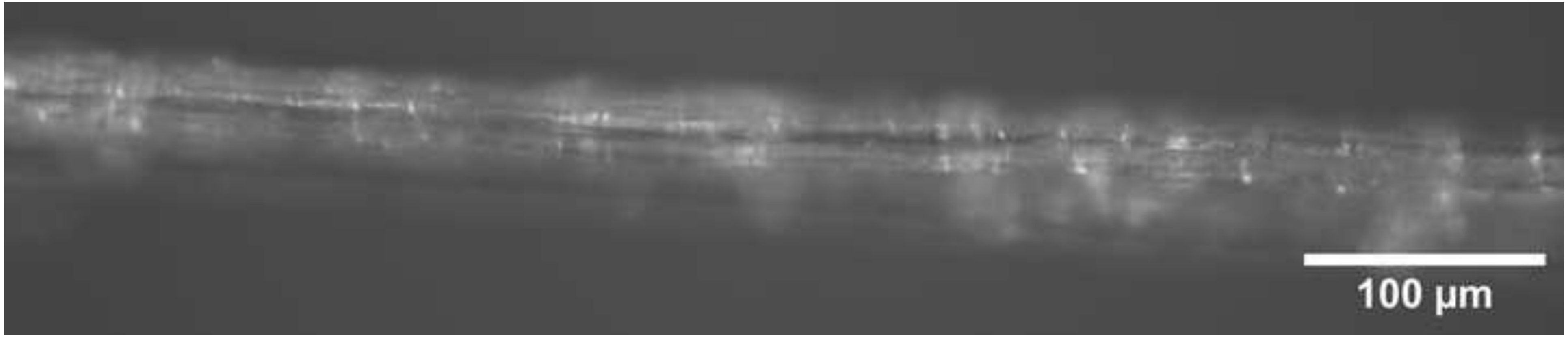

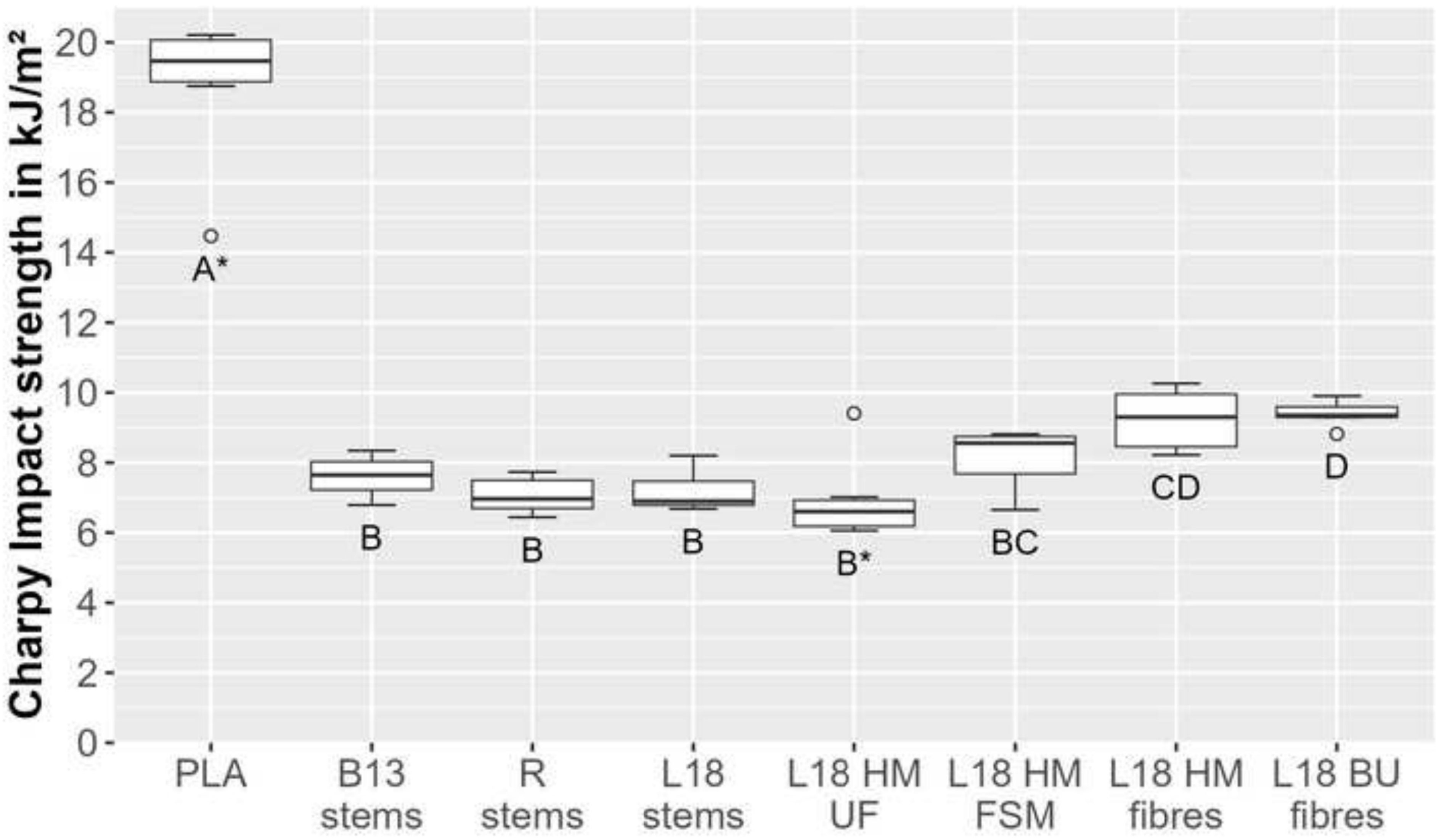
Charpy Impact strength in kJ/m²
20
18
16
14
12
10
8
6
4
2
0
A*
B
B
B
B*
BC
CD
D
PLA
B13 stems
R stems
L18 stems
L18 HM UF
L18 HM FSM
L18 HM fibres
L18 BU fibres